New Journal of Physics
The open–access journal for physics

Analytical solutions for the nonlinear longitudinal drift compression (expansion) of intense charged particle beams

Edward A Startsev and Ronald C Davidson
Plasma Physics Laboratory, Princeton University, Princeton, NJ 08543, USA
E-mail: estartsev@pppl.gov

New Journal of Physics **6** (2004) 141
Received 6 July 2004
Published 26 October 2004
Online at http://www.njp.org/
doi:10.1088/1367-2630/6/1/141

Abstract. To achieve high focal spot intensities in heavy-ion fusion, the ion beam must be compressed longitudinally by factors of 10–100 before it is focused onto the target. The longitudinal compression is achieved by imposing an initial velocity profile tilt on the drifting beam. In this paper, the problem of longitudinal drift compression of intense charged-particle beams is solved analytically for the two important cases corresponding to a cold beam, and a pressure-dominated beam, using a one-dimensional warm-fluid model describing the longitudinal beam dynamics.

PII: S1367-2630(04)83064-7

Contents

1. Introduction **2**
2. Theoretical model **4**
3. General solution **8**
4. General solution of the initial value problem **9**
4.1. Pressure-dominated beam . . . 12
4.2. Cold beam . . . 16
5. Examples with different initial density profiles **18**
5.1. Parabolic density profile . . . 18
5.1.1. Cold beam . . . 18
5.1.2. Pressure-dominated beam . . . 21
5.2. Linear density profile . . . 23
5.2.1. Cold beam . . . 23
5.2.2. Pressure-dominated beam . . . 25
5.3. Flat-top density profile . . . 25
5.3.1. Cold beam . . . 27
5.3.2. Pressure-dominated beam . . . 30
5.4. Continuous density profile (no sharp edge boundary) . . . 31
5.4.1. Cold beam . . . 31
5.4.2. Pressure-dominated beam . . . 32
6. Beam shaping **33**
7. Conclusions **34**
Acknowledgments **35**
Appendix A. Abel transform **35**
References **35**

1. Introduction

High-energy ion accelerators, transport systems and storage rings [1]–[5] have a wide range of applications ranging from basic research in high energy and nuclear physics, to applications such as heavy-ion fusion, spallation neutron sources, and nuclear-waste transmutation. Of particular importance at the high beam currents and charge densities of interest for heavy-ion fusion are the effects of the intense self-fields produced by the beam space charge and current on determining detailed equilibrium, stability, and transport properties. In general, a complete description of collective processes in intense charged-particle beams is provided by the nonlinear Vlasov–Maxwell equations [1] for the self-consistent evolution of the beam distribution function, $f_b(\mathbf{x}, \mathbf{p}, \mathbf{t})$, and the self-generated electric and magnetic fields, $\mathbf{E}(\mathbf{x}, \mathbf{t})$ and $\mathbf{B}(\mathbf{x}, \mathbf{t})$. While considerable progress has been made in analytical and numerical simulation studies of intense beam propagation [6]–[71], the effects of finite geometry and intense self-fields often make it difficult to obtain detailed predictions of beam equilibrium, stability, and transport properties based on the Vlasov–Maxwell equations. To overcome this complexity, considerable theoretical progress has also been made in the development and application of one-dimensional Vlasov–Maxwell models [72]–[79] to describe the longitudinal beam dynamics for a long coasting

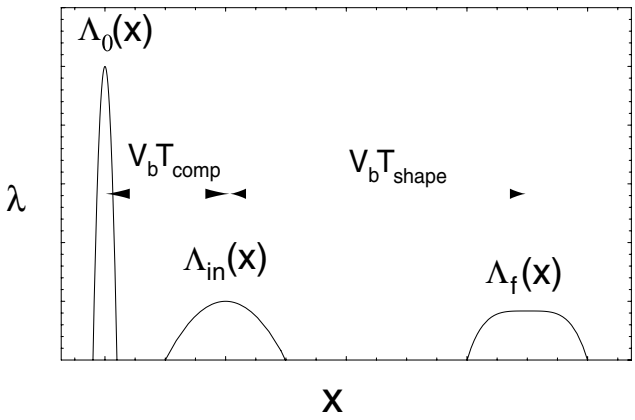

Figure 1. Schematic of the two stages of drift compression described in section 1, the *beam-shaping* stage and the *drift-compression* stage.

beam, with applications ranging from plasma echo excitations, to the investigation of coherent soliton structures, both compressional and rarefactive (hole-like). Such one-dimensional Vlasov descriptions rely on using a geometric-factor (g-factor) model [79]–[85] to incorporate the average effects of the transverse beam geometry and the surrounding wall structure. Despite the many successful applications of such one-dimensional Vlasov models to describe the longitudinal dynamics of long costing beams, even a one-dimensional Vlasov description is often too complicated to be analysed in detail, except in some simple limiting cases. The next level of description of the nonlinear beam dynamics is provided by the macroscopic fluid equations, which correspond to the first three momentum moments of the Vlasov equation, with some particular closure scheme which relates the higher moments to the first three [86]–[90]. The usual closure assumption for collisionless plasma is provided by the adiabatic equation of state ($\mathrm{d}s/\mathrm{d}t = 0$, where s is the entropy per unit volume), which expresses the thermal pressure as a function of the density. In one dimension, this is given by $p\lambda^{-3} = \text{const}$ [86]–[88], where λ is the line density of beam particles and p is the line pressure. Such a one-dimensional fluid model, combined with the adiabatic equation of state and a g-factor model for the average electric field, fits in the class of one-dimensional fluid problems which can be solved exactly [91] using the formalism described in section 2.

In currently envisioned configurations for heavy ion fusion, multiple, high-current, heavy ion beams are focused to a small spot size onto the target capsule. To achieve a high-intensity beam focused onto the target, the beams are first accelerated and then compressed longitudinally. One of the possible ways to compress the beam longitudinally is to use a drift compression scheme illustrated in figure 1 [92]–[101]. The scheme consists of two parts. In the first stage, an initial tilt in the longitudinal velocity profile $-V_f(x)$ is imposed on the long charge bunch with some particular line density profile $\Lambda_f(x)$. After the time T_{shape}, the beam line density evolves to a profile $\Lambda_{in}(x)$, with the velocity profile $-V_{in}(x)$. At this time, an additional velocity tilt $V_{in}(x) - V_{comp}(x)$ is imposed on the beam, and the beam is left with line density $\Lambda_{in}(x)$ and velocity tilt $-V_{comp}(x)$. We refer to this stage as the *beam-shaping* stage. This stage requires beam manipulation (imposing the velocity tilt) and is done when the charge bunch is very long. At this stage, the longitudinal pressure and electric field are negligible, and the beam dynamics is governed by free convection. During this stage the beam may or may not be compressed. The purpose of this stage is to shape the beam line density profile into a certain intermediate line

density profile $\Lambda_{in}(x)$ with velocity profile $-V_{comp}(x)$, such that during the next stage, which we refer to as the *drift-compression* stage, after further axial drift during the time interval T_{comp} (see figure 1), the beam is compressed longitudinally until the space-charge force or the internal thermal pressure stops the longitudinal compression of the charge bunch [92]–[101]. At the point of maximum compression, the velocity tilt profile is completely removed and the beam is left with the desired line density $\Lambda_0(x)$. The final focus magnets then focus the beam onto the target, and the beam heats and compresses the target fuel. Stated this way, the longitudinal drift compression problem in the beam frame is equivalent to the time-reversed problem of the beam expanding into vacuum with zero initial velocity profile, and the specified initial line density profile $\Lambda_0(x)$ which is desired at the time of maximum compression before final focusing. In this paper we employ a one-dimensional warm-fluid model with adiabatic equation of state to study this problem analytically for arbitrary final (maximally compressed) line density profiles $\Lambda_0(x)$.

We consider here the two separate cases corresponding to a cold beam and a pressure-dominated beam. In the case of a cold beam, the internal thermal pressure is negligible, and the dynamics of the drift compression is governed by the self-generated electric field. In the case of a pressure-dominated beam, the self-generated electric field is negligible, and the beam compresses under the influence of the thermal pressure and the initial velocity tilt $-V_{comp}(x)$. One of the compression scenarios considered for heavy ion fusion is *neutralized* drift compression, where the beam propagates through a charge-neutralizing background plasma as it compresses longitudinally. In such a scenario, the beam is compressed only against the internal pressure. For simplicity, the present analysis is carried out in the beam frame where the particle motions are nonrelativistic. The final results can be then Lorentz transformed back to the laboratory frame, moving with axial velocity $-V_b = -\beta_b c$ relative to the average motion of the particles in the beam frame.

This paper is organized as follows. In section 2, we briefly describe the one-dimensional warm-fluid model equations and the formalism used for solving them analytically. In sections 3 and 4, the general solution for the expansion problem (the inverse to the *drift-compression stage* problem) is obtained analytically for the two cases corresponding to a cold beam, and a pressure-dominated beam. In section 5 the general solution to drift compression stage obtained in sections 3 and 4 is illustrated by several examples. In section 6 we briefly discuss the *beam-shaping* stage.

2. Theoretical model

In the present analysis, we employ a one-dimensional warm-fluid model [86]–[88], [93] to describe the longitudinal nonlinear beam dynamics with average electric field given by the g-factor model with $e_b E_z = -e_b^2 g \partial\lambda/\partial x$ [79]–[85]. For example, for a space-charge-dominated beam with flat-top density profile in the transverse plane, $g \simeq 2\ln(r_w/r_b)$ [2, 84, 85]. Here, $\lambda(x, t)$ is the line density, e_b is the charge of a beam particle, r_w is the conducting wall radius, and r_b is the beam radius. Generally, the beam radius, and therefore the g-factor, are functions of the line density and the external transverse focusing, and can change during the beam compression. In most of the drift compression scenarios it is preferable to maintain the beam radius (and therefore the g-factor) constant during the beam compression by adjusting the external transverse focusing [92]–[94]. Therefore, in the present analysis, we assume that the g-factor is a constant.

The macroscopic fluid equations for the line density $\lambda(x, t)$, the average longitudinal beam velocity $v(x, t)$, and the longitudinal line pressure $p(x, t)$ are given by [86]–[88], [93]

$$\frac{\partial \lambda}{\partial t} + \frac{\partial}{\partial x}(\lambda v) = 0, \tag{1}$$

$$\frac{\partial v}{\partial t} + v\frac{\partial}{\partial x}v = -\frac{e_b^2 g}{m_b}\frac{\partial \lambda}{\partial x} - \frac{1}{m_b \lambda}\frac{\partial p}{\partial x} = -\frac{\partial w}{\partial x}, \tag{2}$$

where $p = (p_0/\lambda_0^3)\lambda^3$ for a triple-adiabatic equation of state. Here we have introduced the effective potential w defined by

$$w = c_g^2 \frac{\lambda}{\lambda_0} + \frac{c_p^2}{2}\frac{\lambda^2}{\lambda_0^2}, \tag{3}$$

where $c_g^2 = e_b^2 g \lambda_0 / m_b$ and $c_p^2 = 3p_0/m_b\lambda_0$ are constants with dimensions of (speed)^2, m_b is the mass of a beam particle, and λ_0 and p_0 are constants with the dimensions of line density and line pressure, respectively.

For application in sections 3–6, in the remainder of this section we summarize a well-established theoretical technique developed in fluid mechanics [91] that can be used to solve the nonlinear fluid equations (1) and (2). By introducing the velocity potential ϕ, where $v = \partial\phi/\partial x$, we can rewrite equation (2) as

$$\frac{\partial \phi}{\partial t} + \frac{v^2}{2} + w = 0. \tag{4}$$

The full differential of ϕ then becomes

$$\mathrm{d}\phi = \frac{\partial \phi}{\partial x}\,\mathrm{d}x + \frac{\partial \phi}{\partial t}\,\mathrm{d}t = v\,\mathrm{d}x - \left(\frac{v^2}{2} + w\right)\mathrm{d}t. \tag{5}$$

Next, following Landau and Lifshitz [91], we introduce the Legendre transform

$$\mathrm{d}\phi = \mathrm{d}(xv) - x\,\mathrm{d}v - \mathrm{d}\left[t\left(\frac{v^2}{2} + w\right)\right] + t\,\mathrm{d}\left(\frac{v^2}{2} + w\right). \tag{6}$$

Introducing $\chi = \phi - xv - t(w + v^2/2)$, equation (6) can be expressed as

$$\mathrm{d}\chi = -x\,\mathrm{d}v + t\,\mathrm{d}\left(\frac{v^2}{2} + w\right) = t\,\mathrm{d}w + (vt - x)\,\mathrm{d}v. \tag{7}$$

It follows from equation (7) that χ can be considered as a function of the new independent variables (v, w), and that

$$t = \frac{\partial \chi}{\partial w}, \qquad x - vt = -\frac{\partial \chi}{\partial v}. \tag{8}$$

Therefore, if the function χ is known as a function of its arguments (v, w), then equation (8) gives (v, w) as implicit functions of (x, t).

To obtain the equation for χ we rewrite (1) as

$$\frac{\partial(\lambda, x)}{\partial(t, x)} + v\frac{\partial(t, \lambda)}{\partial(t, x)} + \lambda\frac{\partial(t, v)}{\partial(t, x)} = 0, \tag{9}$$

where

$$\frac{\partial(a, b)}{\partial(x, y)} \equiv \frac{\partial a}{\partial x}\frac{\partial b}{\partial y} - \frac{\partial a}{\partial y}\frac{\partial b}{\partial x}. \tag{10}$$

Assuming that v is not a definite function of w [$v \neq v(w)$], we multiply (9) by $\partial(t, x)/\partial(w, v)$ and use the multiplication property for determinants. This gives

$$\frac{\partial(\lambda, x)}{\partial(w, v)} + v\frac{\partial(t, \lambda)}{\partial(w, v)} + \lambda\frac{\partial(t, v)}{\partial(w, v)} = 0. \tag{11}$$

The case when v is a definite function of w in some region of the (x, t) plane corresponds to *a simple wave* and will be considered later. Because $\lambda = \lambda(w)$, (11) reduces to

$$\frac{\mathrm{d}\lambda}{\mathrm{d}w}\frac{\partial x}{\partial v} - v\frac{\mathrm{d}\lambda}{\mathrm{d}w}\frac{\partial t}{\partial v} + \lambda\frac{\partial t}{\partial w} = 0. \tag{12}$$

Substituting (8) into (12), we obtain the equation for χ [91]

$$\frac{1}{\lambda}\frac{\mathrm{d}\lambda}{\mathrm{d}w}\left(\frac{\partial\chi}{\partial w} - \frac{\partial^2\chi}{\partial v^2}\right) + \frac{\partial^2\chi}{\partial w^2} = 0. \tag{13}$$

Note that (13) is a linear partial differential equation for the function $\chi(v, w)$. By introducing the effective sound speed defined by $c^2 = \lambda\,\mathrm{d}w/\mathrm{d}\lambda$, we can rewrite equation (13) as

$$\frac{\partial\chi}{\partial w} - \frac{\partial^2\chi}{\partial v^2} + c^2\frac{\partial^2\chi}{\partial w^2} = 0, \tag{14}$$

where c^2 is to be regarded as a function of w. Equation (14) together with (8) can be used to obtain the solution to the system of equations (1) and (2) everywhere in the (x, t) plane except in the regions corresponding to *simple wave* solutions where $v = v(c)$ [91]. In this case, the Jacobian $\Delta = \partial(v, w)/\partial(x, t)$ vanishes identically. In deriving (11), we divided (9) by this Jacobian, and the solution for which $\Delta = 0$ is not recovered. Thus, a simple wave solution cannot be recovered from the general equation (13).

If v is a function of λ only, as in a simple wave, we can rewrite (1) and (2) as [91]

$$\frac{\partial\lambda}{\partial t} + \frac{\mathrm{d}(\lambda v)}{\mathrm{d}\lambda}\frac{\partial\lambda}{\partial x} = 0, \tag{15}$$

$$\frac{\partial v}{\partial t} + \left(v + \frac{\mathrm{d}w}{\mathrm{d}v}\right)\frac{\partial v}{\partial x} = 0. \tag{16}$$

Since

$$\frac{\partial\lambda/\partial t}{\partial\lambda/\partial x} = -\left(\frac{\partial x}{\partial t}\right)_\lambda, \qquad \frac{\partial v/\partial t}{\partial v/\partial x} = -\left(\frac{\partial x}{\partial t}\right)_v,$$

we obtain from equations (15) and (16)

$$\left(\frac{\partial x}{\partial t}\right)_{\lambda} = v + \lambda \frac{\mathrm{d}v}{d\lambda}, \tag{17}$$

$$\left(\frac{\partial x}{\partial t}\right)_{v} = v + \frac{\mathrm{d}w}{\mathrm{d}v}. \tag{18}$$

However, because $v = v(\lambda)$, it follows that $(\partial x/\partial t)_{\lambda} = (\partial x/\partial t)_{v}$, so that $\lambda\,\mathrm{d}v/\mathrm{d}\lambda = \mathrm{d}w/\mathrm{d}v = (\mathrm{d}w/\mathrm{d}\lambda)(\mathrm{d}\lambda/\mathrm{d}v) = (c^2/\lambda)\,\mathrm{d}\lambda/\mathrm{d}v$, and therefore

$$v = \pm \int \frac{c}{\lambda}\,\mathrm{d}\lambda. \tag{19}$$

Next, we combine equations (17), (18) and (19) to give $(\partial x/\partial t)_{v} = (\partial x/\partial t)_{\lambda} = v + \lambda(\mathrm{d}v/\mathrm{d}\lambda) = v \pm c(v)$. Integrating with respect to t then gives [91]

$$x = t[v \pm c(v)] + f(v), \tag{20}$$

where $f(v)$ is an arbitrary function of the velocity v determined from the initial conditions, and $c(v)$ is given by (19).

Equations (19) and (20) give the general solution for the *simple wave*. The two signs in (19) and (20) correspond to the direction of wave propagation: (+) is for a wave propagating in the positive x direction, and (−) is for a wave propagating in the negative x direction.

It is also convenient to solve (1) and (2) using the method of *characteristics* [91]. Multiplying (1) by c/λ, and then adding and subtracting from (2), and making use of the relation $\partial w/\partial x = (\mathrm{d}w/\mathrm{d}\lambda)(\partial\lambda/\partial x) = (c^2/\lambda)(\partial\lambda/\partial x)$, we obtain

$$\frac{\partial v}{\partial t} \pm \frac{c}{\lambda}\frac{\partial \lambda}{\partial t} + (v \pm c)\left(\frac{\partial v}{\partial x} \pm \frac{c}{\lambda}\frac{\partial \lambda}{\partial x}\right) = 0. \tag{21}$$

We now introduce the new unknown functions

$$J_{+} = v + \int \frac{c}{\lambda}\,\mathrm{d}\lambda, \qquad J_{-} = v - \int \frac{c}{\lambda}\,\mathrm{d}\lambda, \tag{22}$$

which are called *Riemann invariants*. In terms of J_{+} and J_{-}, the equations of motion take the simple form [91]

$$\left[\frac{\partial}{\partial t} + (v + c)\frac{\partial}{\partial x}\right] J_{+} = 0, \qquad \left[\frac{\partial}{\partial t} + (v - c)\frac{\partial}{\partial x}\right] J_{-} = 0. \tag{23}$$

The differential operators acting on J_{+} and J_{-} are the operators for differentiation along the curves C_{+} and C_{-} (called *characteristics*) in the (x, t) plane given by the equations

$$C_{+}: \frac{\mathrm{d}x}{\mathrm{d}t} = v + c, \qquad C_{-}: \frac{\mathrm{d}x}{\mathrm{d}t} = v - c. \tag{24}$$

The values of v and c at every point of the (x, t) plane are given by the values of the Riemann invariants J_{+} and J_{-} which are transported to this point along the C_{+} and C_{-} characteristics from

the region where the values of J_+ and J_- (and therefore v and c) are known. Equations (22) and (24) are very convenient for numerical solution of the equations of motion and also for the general analysis of the flow.

The totality of the available space–time generally consists of the regions where either a simple wave solution (equation (20)) or a general solution (solution to equation (14) together with (8)) is applicable. The boundary between the simple wave solution and the general solution, like any boundary between two analytically different solutions, is a characteristic [91]. In solving particular problems (see section 5), the value of the function $\chi(v, w)$ on this boundary characteristic must be determined. The matching condition at the boundary between the simple wave solution and the general solution is obtained by substituting (8) for x and t into the equation for the simple wave (equation (20)). This gives

$$\frac{\partial \chi}{\partial v} \pm c\frac{\partial \chi}{\partial w} + f(v) = 0. \tag{25}$$

Moreover, in the simple wave solution (and therefore on the boundary characteristic), we obtain $\mathrm{d}w/\mathrm{d}v = (\mathrm{d}w/\mathrm{d}\lambda)(\mathrm{d}\lambda/\mathrm{d}v) = (c^2/\lambda)(\mathrm{d}\lambda/\mathrm{d}v) = \pm c$. Substituting into (25) then gives

$$\frac{\partial \chi}{\partial v} + \frac{\mathrm{d}w}{\mathrm{d}v}\frac{\partial \chi}{\partial w} + f(v) = \frac{\mathrm{d}\chi}{\mathrm{d}v} + f(v) = 0. \tag{26}$$

Equation (26) can be integrated to give [91]

$$\chi = -\int f(v)\,\mathrm{d}v, \tag{27}$$

which determines the required boundary value of χ.

3. General solution

Here we consider two separate cases. For the case of a cold beam ($p_0 = 0$ and $c_p^2 = 0$) it follows that $w = c_g^2(\lambda/\lambda_0)$ (equation (3)), and $c^2(w) = \lambda\,\mathrm{d}w/\mathrm{d}\lambda = w$. In the opposite limit corresponding to a pressure-dominated beam, where we can neglect the electric field compared to the thermal pressure, it follows that $w = (c_p^2/2)(\lambda/\lambda_0)^2$, and $c^2(w) = \lambda\,\mathrm{d}w/\mathrm{d}\lambda = 2w$. Introducing in place of w the variable $c = \sqrt{nw}$, where $n = 1, 2$, we can rewrite (14) as

$$\frac{\partial^2 \chi^{n=1}}{\partial c^2} + \frac{1}{c}\frac{\partial \chi^{n=1}}{\partial c} - 4\frac{\partial^2 \chi^{n=1}}{\partial v^2} = 0, \quad \text{for } n = 1, \tag{28}$$

$$\frac{\partial^2 \chi^{n=2}}{\partial c^2} - \frac{\partial^2 \chi^{n=2}}{\partial v^2} = 0, \quad \text{for } n = 2. \tag{29}$$

Equation (29) is an ordinary wave equation whose general solution is

$$\chi^{n=2}(v, c) = f_1(c + v) + f_2(c - v), \tag{30}$$

where f_1 and f_2 are arbitrary functions. To find the general solution to (28) we first Fourier transform with respect to the v dependence. This gives

$$\frac{\partial^2 \chi_k^{n=1}}{\partial c^2} + \frac{1}{c}\frac{\partial \chi_k^{n=1}}{\partial c} - 4k^2\chi_k^{n=1} = 0. \tag{31}$$

Equation (31) is Bessel's equation of order zero which has two Hankel functions, $H_0^{(1)}(2kc)$ and $H_0^{(2)}(2kc) = [H_0^{(1)}(2kc)]^*$, as independent solutions. Here (*) represents complex conjugate. Using the integral representation of the Hankel function [102],

$$H_0^{(1)}(x) = -2i \int_1^\infty \frac{e^{ixt}}{\sqrt{t^2-1}}\,dt, \tag{32}$$

the general solution to (28) can be expressed as

$$\chi^{n=1}(v,c) = \int_{-\infty}^{\infty} dk \int_1^\infty dt A(k) \frac{e^{i(2ct-v)k}}{\sqrt{t^2-1}} + \int_{-\infty}^{\infty} dk \int_1^\infty dt\, B(k) \frac{e^{i(2ct+v)k}}{\sqrt{t^2-1}}, \tag{33}$$

where $A(k)$ and $B(k)$ are arbitrary functions. Finally, we can rewrite (33) as

$$\chi^{n=1}(v,c) = \int_1^\infty \frac{dt}{\sqrt{t^2-1}} [f_1(tc - v/2) + f_2(tc + v/2)], \tag{34}$$

where f_1 and f_2 are arbitrary functions such that the integrals in (34) converge. Equation (34) provides the general solution to (28).

In the regions pertaining to the simple wave solution, (19) gives the general relation between velocity and the density or sound speed in the wave. In the two cases considered here, $\lambda/\lambda_0 = (c/c_g)^2$ for a cold beam ($n = 2$), and $\lambda/\lambda_0 = c/c_p$ for a pressure-dominated beam ($n = 1$). For these two cases, we find

$$v = \pm c + a, \qquad n = 1, \tag{35}$$

$$v = \pm 2c + a, \qquad n = 2, \tag{36}$$

where a is a constant. Equations (35) and (36) together with (20) give a simple wave solution for the two cases considered in this section. From (22), the corresponding Riemann invariants can be expressed as

$$J_+^{n=1} = v + c, \qquad J_-^{n=1} = v - c \quad (n = 1), \tag{37}$$

$$J_+^{n=2} = v + 2c, \qquad J_-^{n=2} = v - 2c \quad (n = 2). \tag{38}$$

4. General solution of the initial value problem

In this section we make use of (30) and (34) to solve the initial value problem for the case of beam expansion into vacuum. The initial conditions for this problem are zero flow velocity at every point, $v_0(x, 0) = 0$, and prescribed density profile $\lambda(x, 0) = \lambda_0(x)$, which expresses the initial line density as a function of x. At some later time $t = t_f$, the density and velocity profiles will be given by the functions $\lambda(x, t_f)$ and $v(x, t_f)$ which are the solutions to (1) and (2). Since the equations of motion (equations (1) and (2)) are time-reversible, the flow described by $\bar{\lambda}(x, t) = \lambda(x, t_f - t)$ and $\bar{v}(x, t) = -v(x, t_f - t)$ are also solutions to these equations with initial conditions $\bar{v}(x, 0) = -v(x, t_f)$ and $\bar{\lambda}(x, 0) = \lambda(x, t_f)$. At time $t = t_f$, this flow has zero

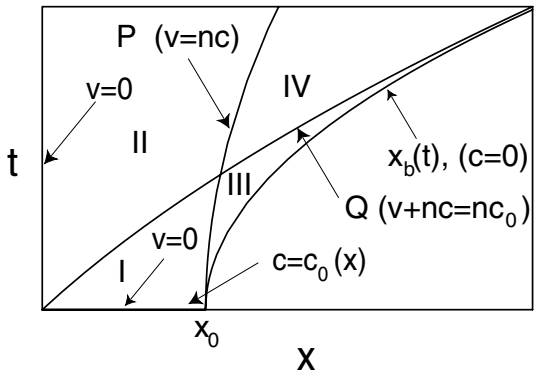

Figure 2. The area in the (x, t) plane occupied by the four regions of flow.

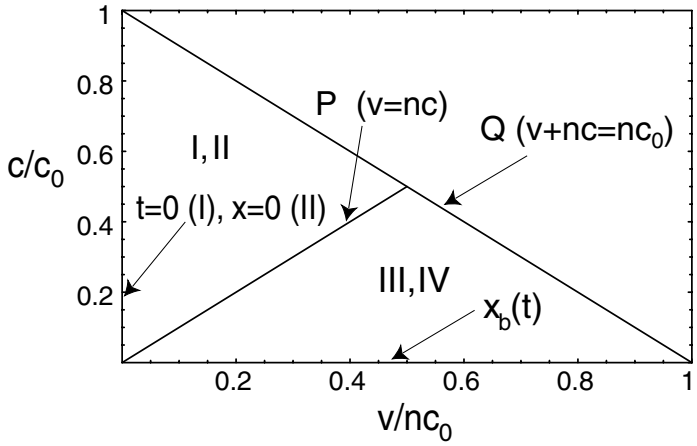

Figure 3. The area in the (v, c) plane occupied by the four regions of flow.

velocity profile ($\bar{v} = 0$) and the density profile is given by the initial profile for the expansion problem, i.e., $\bar{\lambda}(x, t_f) = \lambda_0(x)$.

To solve the initial value problem we assume that the density profile $\lambda_0(x)$, or equivalently the sound velocity profile $c_0(x)$, decreases monotonically to zero at the beam boundary $x = \pm x_0$, is an even function of x, and is an invertible function for $x > 0$ everywhere where the density is non-zero. Therefore, we assume that at $t = 0$ the inverted profile $x_0(c)$ is known. The condition that $c_0(x)$ decreases monotonically to zero at the beam boundary means that no rarefaction wave is launched from the boundary into the beam as it expands. We will treat the case with discontinuities in $c_0(x)$ at the beam boundary in one of the examples in section 5. Since we are interested in the time-reversed problem of beam compression, we assume that multi-valued flow does not form as the beam expands. This is equivalent to considering only initial density profiles with first derivative decreasing continuously from the beam centre to the beam edge. This guarantees that the portions of the beam with smaller density accelerate faster than the portions with larger density, and as a result, the flow is never multi-valued. We will treat the case with multi-valued flow in one of the examples in section 5. The region of flow in the (x, t) plane and its boundaries are illustrated in figure 2. It is obvious that the flow is symmetric under reflection, $x \to -x$, and therefore we need only to solve the equations in the region $x > 0$. In general, there are four regions of flow (see figures 2 and 3).

Each is separated from the others by two characteristics, the C_- characteristic P on which $v = nc$, and the C_+ characteristic Q on which $v + nc = nc_0$. The boundary conditions are given by

$$v(0, t) = 0, \quad c(x, 0) = c_0(x), \quad v(x, 0) = 0, \quad \text{for } |x| < x_0, \quad c[x_b(t), t] = 0, \tag{39}$$

where $x_0 = x_b(t = 0)$ is the initial beam half-width, and $x_b(t)$ is the coordinate of the beam edge.

As is evident from figure 2, the flow at every point in region I is brought to this point by the characteristics originating from the x-axis at $t = 0$. Hence, the flow in this region is fully determined by the boundary conditions $c(x, 0) = c_0(x)$ and $v(x, 0) = 0$. The flow at every point in region II, which is separated from region I by the C_+ characteristic Q originating from the origin in the (x, t) plane, is brought to this point by the characteristics originating from the $x = 0$ line where $v(0, t) = 0$, and from region I. Therefore, the boundary condition for region II is given by $v(0, t) = 0$ and by the flow on the separating characteristic Q. The flow at every point in region III, which is adjacent to the beam edge and separated from region I by the C_- characteristic P originating from the beam edge at $t = 0$ in the (x, t) plane, is brought to this point by the characteristics originating from the beam edge where $c[x_b(t), t] = 0$, and from region I. Therefore, the boundary condition for region III is given by $c[x_b(t), t] = 0$ and by the flow on the separating characteristic P. The flow at every point in region IV, which is separated from region II by the P characteristic and from region III by the Q characteristic, is brought to this point by the characteristics originating from region II and region III. Therefore the boundary condition for region IV is given by the flow on the separating characteristics P and Q.

The function $\chi(v, c)$ and equation (8) provide the map of the flow region in the (x, t) plane illustrated in figure 2, to the (v, c) plane (figure 3). The region is a triangle $(0 < c < c_0)$ limited from above by the C_+ characteristic Q which is a straight line in the (v, c) plane since on this characteristic $J_+ = v + nc = nc_0 = \text{const}\ (n = 1, 2)$. This mapping is not one-to-one. In fact, regions I and II and regions III and IV in the (x, t) plane map into the same regions in the (v, c) plane, which means that in the (v, c) plane there will be four functions, χ^{I}, χ^{II}, χ^{III} and χ^{IV}, defined inside the area depicted in figure 3, which map the depicted (v, c) region back into regions I, II, III and IV in the (x, t) plane, respectively, by means of equation (8).

Since at $t = 0$, $v(x, 0) = 0$ and $c(x, 0) = c_0(x)$, by making use of equation (8) we obtain the boundary conditions for $\chi^{\mathrm{I}}(v, c)$ in the (v, c) plane in region I, which can be expressed as

$$t = 0 = \left(\frac{\partial \chi^{\mathrm{I}}}{\partial w}\right)_{v=0} = 0, \quad \text{or equivalently,} \quad \left(\frac{\partial \chi^{\mathrm{I}}}{\partial c}\right)_{v=0} = 0, \tag{40}$$

$$x_0(c) = -\left(\frac{\partial \chi^{\mathrm{I}}}{\partial v}\right)_{v=0}. \tag{41}$$

Since $v(0, t) = 0$ at $x = 0$, the boundary condition for $\chi^{\mathrm{II}}(v, c)$ is

$$\left(\frac{\partial \chi^{\mathrm{II}}}{\partial v}\right)_{v=0} = 0. \tag{42}$$

The second boundary condition for $\chi^{\mathrm{II}}(v, c)$ reflects continuity of the mapping in equation (8),

$$\left(\frac{\partial \chi^{\mathrm{II}}}{\partial v}\right)_{v+nc=nc_0} = \left(\frac{\partial \chi^{\mathrm{I}}}{\partial v}\right)_{v+nc=nc_0}, \tag{43}$$

$$\left(\frac{\partial \chi^{\mathrm{II}}}{\partial c}\right)_{v+nc=nc_0} = \left(\frac{\partial \chi^{\mathrm{I}}}{\partial c}\right)_{v+nc=nc_0}. \tag{44}$$

By making use of $c[x_b(t), t] = 0$, the definition $c^2 = \lambda\, \mathrm{d}w/\mathrm{d}\lambda = nw$ and equation (8), we obtain the boundary condition for $\chi^{\mathrm{III}}(v, c)$,

$$\left(\frac{\partial \chi^{\mathrm{III}}}{\partial c}\right)_{c=0} = 0. \tag{45}$$

The second boundary condition for $\chi^{\mathrm{III}}(v, c)$ reflects continuity of the mapping in equation (8),

$$\left(\frac{\partial \chi^{\mathrm{III}}}{\partial v}\right)_{v=nc} = \left(\frac{\partial \chi^{\mathrm{I}}}{\partial v}\right)_{v=nc}, \tag{46}$$

$$\left(\frac{\partial \chi^{\mathrm{III}}}{\partial c}\right)_{v=nc} = \left(\frac{\partial \chi^{\mathrm{I}}}{\partial c}\right)_{v=nc}. \tag{47}$$

Finally, the boundary conditions for $\chi^{\mathrm{IV}}(v, c)$ reflects continuity of the mapping in equation (8),

$$\left(\frac{\partial \chi^{\mathrm{IV}}}{\partial v}\right)_{v+nc=nc_0} = \left(\frac{\partial \chi^{\mathrm{III}}}{\partial v}\right)_{v+nc=nc_0}, \tag{48}$$

$$\left(\frac{\partial \chi^{\mathrm{IV}}}{\partial c}\right)_{v+nc=nc_0} = \left(\frac{\partial \chi^{\mathrm{III}}}{\partial c}\right)_{v+nc=nc_0}, \tag{49}$$

and

$$\left(\frac{\partial \chi^{\mathrm{IV}}}{\partial v}\right)_{v=nc} = \left(\frac{\partial \chi^{\mathrm{II}}}{\partial v}\right)_{v=nc}, \tag{50}$$

$$\left(\frac{\partial \chi^{\mathrm{IV}}}{\partial c}\right)_{v=nc} = \left(\frac{\partial \chi^{\mathrm{II}}}{\partial c}\right)_{v=nc}. \tag{51}$$

Next, we consider separately the two cases corresponding to a cold beam, and a pressure-dominated beam.

4.1. Pressure-dominated beam

The general solution for the case of a pressure-dominated beam is given by (30). To satisfy the boundary condition in (40), we are required to choose

$$\chi^{\mathrm{I}} = f(c - v) - f(c + v). \tag{52}$$

Substituting (52) into (41), we obtain $f'(c) = x_0(c)/2$, and therefore

$$f(c) = \frac{1}{2}\int_{c_0}^{c} x_0(\bar{c})\,\mathrm{d}\bar{c}. \tag{53}$$

Here, we have chosen the integration constant so that $f(c_0) = 0$. Substituting (53) into (52) then gives

$$\chi^{\mathrm{I}} = \frac{1}{2}\int_{c+v}^{c-v} x_0(\bar{c})\,\mathrm{d}\bar{c}. \tag{54}$$

In region II, to satisfy the boundary conditions in (42), we are required to choose

$$\chi^{\mathrm{II}} = g(c-v) + g(c+v). \tag{55}$$

To satisfy the boundary conditions in (43) and (44) we choose $g(c) = f(c)$. Hence, the solution in region II is given by

$$\chi^{\mathrm{II}} = \frac{1}{2}\left(\int_{c_0}^{c-v} x_0(\bar{c})\,\mathrm{d}\bar{c} + \int_{c_0}^{c+v} x_0(\bar{c})\,\mathrm{d}\bar{c}\right). \tag{56}$$

It is readily shown that the solution in region III which satisfies all the boundary conditions in (45)–(47) is given by

$$\chi^{\mathrm{III}} = -\frac{1}{2}\left(\int_{c_0}^{v-c} x_0(\bar{c})\,\mathrm{d}\bar{c} + \int_{c_0}^{c+v} x_0(\bar{c})\,\mathrm{d}\bar{c}\right), \tag{57}$$

and the solution in region IV which satisfies all of the boundary conditions in equations (48)–(51) is given by

$$\chi^{\mathrm{IV}} = \frac{1}{2}\int_{v-c}^{c+v} x_0(\bar{c})\,\mathrm{d}\bar{c}. \tag{58}$$

Finally, using equation (8) and the definition $c^2 = \lambda\,\mathrm{d}w/\mathrm{d}\lambda = 2w$, we obtain the solutions in region I,

$$x - vt = \frac{1}{2}[x_0(c-v) + x_0(c+v)], \qquad t = \frac{1}{2c}[x_0(c-v) - x_0(c+v)], \tag{59}$$

in region II,

$$x - vt = \frac{1}{2}[x_0(c-v) - x_0(c+v)], \qquad t = \frac{1}{2c}[x_0(c-v) + x_0(c+v)]. \tag{60}$$

in region III,

$$x - vt = \frac{1}{2}[x_0(v-c) + x_0(c+v)], \qquad t = \frac{1}{2c}[x_0(v-c) - x_0(c+v)], \tag{61}$$

and in region IV,

$$x - vt = \frac{1}{2}[x_0(v-c) - x_0(c+v)], \qquad t = \frac{1}{2c}[x_0(v-c) + x_0(c+v)]. \tag{62}$$

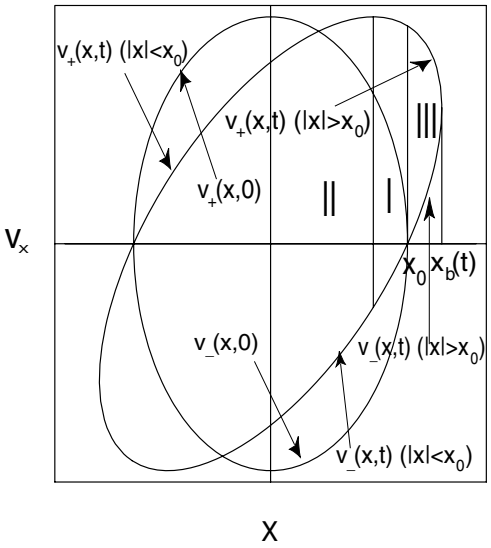

Figure 4. Schematic in (x, v_x) phase space of the flow for a pressure-dominated beam.

Equations (59) and (60) give the implicit solution for describing the expansion of a pressure-dominated beam. We can also obtain the formulae for the asymptotic solution as $t \to \infty$ or $c \to 0$. Indeed, for $t \to \infty$ or $c \to 0$ the flow is almost entirely in region IV. Using equation (62), we obtain

$$t = \frac{1}{c}\frac{\partial \chi^{\mathrm{IV}}}{\partial c} = \frac{x_0(v)}{c} + \frac{x''(v)c}{2} + O(c^3), \qquad x - vt = -\frac{\partial \chi^{\mathrm{IV}}}{\partial v} = -x_0'(v)c + O(c^3). \tag{63}$$

Finally, in the leading approximation, we can rewrite (63) as

$$\frac{\lambda(x,t)}{\lambda_0} = \frac{1}{c_0 t} x_0\left(\frac{x}{t}\right), \qquad v(x,t) = \frac{x}{t}, \quad \text{for } t \to \infty. \tag{64}$$

Evidently, the density profile given by (64) is correctly normalized.

The same solution can be also obtained from a kinetic description. It has been shown in [88] that equations (1) and (2) (together with the adiabatic pressure relation $p = p_0(\lambda/\lambda_0)^3$) are the two key moments of the kinetic Vlasov equation for a waterbag distribution function ($f = \text{const}$ in an enclosed area of phase space). Indeed if we denote the upper curve in figure 4 as $v_+(x,t)$ and the lower curve as $v_-(x,t)$, then by multiplying the Vlasov equation for $f(x, v_x, t)$

$$\frac{\partial f}{\partial t} + v_x \frac{\partial f}{\partial x} = 0, \tag{65}$$

by 1 and by v_x, integrating over v_x, and keeping in mind that $f = \text{const}$ inside the region limited from above by $v_+(x,t)$ and from below by $v_-(x,t)$, we obtain

$$\frac{\partial}{\partial t}[v_+(x,t) - v_-(x,t)] + \frac{1}{2}\frac{\partial}{\partial x}[v_+(x,t)^2 - v_-(x,t)^2] = 0, \tag{66}$$

$$\frac{1}{2}\frac{\partial}{\partial t}[v_+(x,t)^2 - v_-(x,t)^2] + \frac{1}{3}\frac{\partial}{\partial x}[v_+(x,t)^3 - v_-(x,t)^3] = 0. \tag{67}$$

Introducing the line density and flow velocity defined by

$$\lambda(x,t) = \frac{\lambda_0}{[v_+(0,0) - v_-(0,0)]}[v_+(x,t) - v_-(x,t)], \tag{68}$$

$$v(x,t) = \tfrac{1}{2}[v_+(x,t) + v_-(x,t)], \tag{69}$$

where λ_0 is the density at $x = 0$ at $t = 0$, we can rewrite the equations (66) and (67) in the familiar form

$$\frac{\partial}{\partial t}\lambda(x,t) + \frac{\partial}{\partial x}[\lambda(x,t)v(x,t)] = 0, \tag{70}$$

$$\frac{\partial}{\partial t}[\lambda(x,t)v(x,t)] + \frac{\partial}{\partial x}[\lambda(x,t)v(x,t)^2] + \frac{1}{12}\frac{[v_+(0,0) - v_-(0,0)]^2}{\lambda_0^2}\frac{\partial}{\partial x}\lambda(x,t)^3 = 0. \tag{71}$$

Comparing with (2), we obtain $c^2 = \lambda\, \mathrm{d}w/\mathrm{d}\lambda = ([v_+(0,0) - v_-(0,0)]^2/4\lambda_0^2)\lambda^2$, or $c(x,t) = ([v_+(0,0) - v_-(0,0)]/2\lambda_0)\lambda(x,t) = (1/2)[v_+(x,t) - v_-(x,t)]$. Therefore, $v_+(x,t) = c(x,t) + v(x,t)$ and $v_-(x,t) = v(x,t) - c(x,t)$. If the initial profiles are given by $v(x,0) = 0$ and $c(x,0) = c_0(x)$, then $v_+(x,0) = c_0(x)$ and $v_-(x,0) = -c_0(x)$. Since (65) represents the free-streaming motion of the particles in phase space along straightline trajectories, we readily obtain the expressions for $v_-(x,t)$ and $v_+(x,t)$,

$$v_+(x,t) = c_0[x - v_+(x,t)t], \tag{72}$$

$$v_-(x,t) = \pm c_0[x - v_-(x,t)t]. \tag{73}$$

Here, the '$-$' sign in (73) holds for $|x| < x_0$ (x_0 is the coordinate of the beam edge at $t = 0$) and corresponds to regions I and II in figure 2, and the '+' sign holds for $x_b(t) > |x| > x_0$ and corresponds to regions III and IV in figure 2 (see figure 4). Equations (72) and (73) can be rewritten as equations for $c(x,t)$ and $v(x,t)$,

$$c(x,t) = \tfrac{1}{2}\{c_0[x - (v+c)t] \pm c_0[x - (v-c)t]\}, \tag{74}$$

$$v(x,t) = \tfrac{1}{2}\{c_0[x - (v+c)t] \mp c_0[x - (v-c)t]\}. \tag{75}$$

By adding and subtracting (74) and (75), and inverting the resulting equations, we obtain

$$\pm x_0(v+c) = x - (v+c)t, \tag{76}$$

$$x_0(c-v) = x - (v-c)t, \tag{77}$$

for regions I and II, and

$$\pm x_0(v+c) = x - (v+c)t, \tag{78}$$

$$x_0(v-c) = x - (v-c)t, \tag{79}$$

for regions III and IV, respectively. The '+' sign in (76)–(79) corresponds to region I (equations (76) and (77)) and region III (equations (78) and (79)), and the '$-$' sign corresponds to region II (equations (76) and (77)) and region IV (equations (78) and (79)) (see figures 2 and 4). The $\pm$ signs appear here because we have assumed an even initial profile $c_0(-x) = c_0(x)$.

Finally, by adding and subtracting, equations (76)–(79) take the form shown in equations (59)–(62).

4.2. Cold beam

Here we use the general solution in (34) to solve the same initial value problem as discussed in the previous section, applied now to the case of a cold beam. To satisfy the boundary condition in (40) we are required to choose

$$\chi^{\mathrm{I}}(v,c) = \int_1^\infty \frac{\mathrm{d}t}{\sqrt{t^2-1}}[f(tc+v/2) - f(tc-v/2)]. \tag{80}$$

Substituting (80) into (41), we obtain

$$x_0(c) = -\left(\frac{\partial \chi^{\mathrm{I}}}{\partial v}\right)_{v=0} = -\int_c^\infty \frac{\mathrm{d}z}{\sqrt{z^2-c^2}}\frac{\mathrm{d}f(z)}{\mathrm{d}z}. \tag{81}$$

Equation (81) can be inverted by using the integral Abel transform in appendix A. This gives

$$f(z) = \frac{2}{\pi}\int_z^{c_0} \frac{qx_0(q)\,\mathrm{d}q}{\sqrt{q^2-z^2}}\Theta(z<c_0), \tag{82}$$

where $c_0 = c_0(x=0)$, $\Theta(z<a)$ is the Heaviside step-function, and $z>0$. Note from (80) that in regions I and II, where $v<2c$, the argument of f in (80) is positive, and we can use the form of f defined in (82). For $v>2c$ (regions III and IV), the argument of the function under the integral in the first term in the general solution in (34) can become negative. Next, we show that the solution of the form in (80) with $f(z)$ continued to the regions where $z<0$ as $f(z)=f(-z)$, or $f(z)=f(|z|)$, will satisfy the boundary conditions in (45)–(47). Indeed, by expanding f in a Taylor series in (80) for $c\to 0$, we obtain

$$I^- = \int_1^{(c_0+v/2)/c} \frac{\mathrm{d}t}{\sqrt{t^2-1}} f(tc-v/2) = \left[f(-v/2) + \frac{c^2}{4}f''(-v/2)\right]\ln\left(\frac{c_0}{c}\right) - q(v) + O(c^2), \tag{83}$$

and therefore

$$\chi^{\mathrm{III}} = f(v/2)\ln\left(\frac{c_0}{c}\right) - f(-v/2)\ln\left(\frac{c_0}{c}\right) + p(v) + O\left[c^2\ln\left(\frac{c_0}{c}\right)\right], \tag{84}$$

where $q(v)$ and $p(v)=q(v)-q(-v)$ are functions of v alone. Differentiating with respect to c, and taking the limit $c\to 0$ in (84), we obtain

$$\left(\frac{\partial \chi^{\mathrm{III}}}{\partial c}\right)_{c\to 0} = \frac{[f(-v/2)-f(v/2)]}{c} + O\left[c\ln\left(\frac{c_0}{c}\right)\right] = 0, \tag{85}$$

provided $f=f(|z|)$. It readily follows that the continuity conditions in (46)–(47) are also satisfied. Therefore, the solutions in regions I and III are given by

$$\chi^{\mathrm{I,III}}(v,c) = \int_1^\infty \frac{\mathrm{d}t}{\sqrt{t^2-1}}[f(tc+v/2) - f(tc-v/2)], \tag{86}$$

where

$$f(z) = \frac{2}{\pi}\int_{|z|}^{c_0} \frac{qx_0(q)\,\mathrm{d}q}{\sqrt{q^2-z^2}}\Theta(|z|<c_0). \tag{87}$$

To obtain the solutions in regions II and IV, we note that the function

$$\chi^{\mathrm{II,IV}}(v,c) = -\int_1^\infty \frac{\mathrm{d}t}{\sqrt{t^2-1}}[f(tc+v/2)+f(tc-v/2)] \tag{88}$$

satisfies the condition in (42). Also, if we choose f as in (87), the second term (and its first derivatives) in both equations (80) and (88) is zero on the dividing characteristic $2c+v=2c_0$, and therefore all of the continuity conditions in (48)–(51) are also satisfied. Equations (86)–(88) together with (8) give the formal solution of the expansion problem for the case of a cold beam. Finally, substituting (87) into (86) and (88), changing the order of integration, and performing the integrations, we obtain

$$\chi^{\mathrm{I}}(v,c) = -\frac{2c}{\pi}\int_{1-v/2c}^{1+v/2c} \mathrm{d}q\sqrt{q}x_0(cq)K\left[\frac{(v/2c)^2-(q-1)^2}{4q}\right], \tag{89}$$

$$\begin{aligned}\chi^{\mathrm{II}}(v,c) = &-\frac{2c}{\pi}\int_{1-v/2c}^{1+v/2c} \mathrm{d}q\sqrt{q}x_0(cq)K\left[\frac{(v/2c)^2-(q-1)^2}{4q}\right]\\ &-\frac{8c}{\pi}\int_{1+v/2c}^{c_0/c}\frac{\mathrm{d}q\,qx_0(cq)}{\sqrt{(q+1)^2-(v/2c)^2}}K\left[\frac{(q-1)^2-(v/2c)^2}{(q+1)^2-(v/2c)^2}\right],\end{aligned} \tag{90}$$

$$\begin{aligned}\chi^{\mathrm{III}}(v,c) = &-\frac{2c}{\pi}\int_{v/2c-1}^{1+v/2c} \mathrm{d}q\sqrt{q}x_0(cq)K\left[\frac{(v/2c)^2-(q-1)^2}{4q}\right]\\ &-\frac{4c}{\pi}\int_0^{v/2c-1}\frac{\mathrm{d}q\,qx_0(cq)}{\sqrt{(v/2c)^2-(q-1)^2}}K\left[\frac{4q}{(v/2c)^2-(q-1)^2}\right],\end{aligned} \tag{91}$$

$$\begin{aligned}\chi^{\mathrm{IV}}(v,c) = &-\frac{2c}{\pi}\int_{v/2c-1}^{1+v/2c} \mathrm{d}q\sqrt{q}x_0(cq)K\left[\frac{(v/2c)^2-(q-1)^2}{4q}\right]\\ &-\frac{4c}{\pi}\int_0^{v/2c-1}\frac{\mathrm{d}q\,qx_0(cq)}{\sqrt{(v/2c)^2-(q-1)^2}}K\left[\frac{4q}{(v/2c)^2-(q-1)^2}\right]\\ &-\frac{8c}{\pi}\int_{1+v/2c}^{c_0/c}\frac{\mathrm{d}q\,qx_0(cq)}{\sqrt{(q+1)^2-(v/2c)^2}}K\left[\frac{(q-1)^2-(v/2c)^2}{(q+1)^2-(v/2c)^2}\right].\end{aligned} \tag{92}$$

Here, K is the complete elliptic integral of the first kind [102]. In section 5, we illustrate the application of these solutions with several examples.

We can also obtain the formulas for the asymptotic solution as $t\to\infty$ or $c\to 0$. Indeed, for $t\to\infty$ or $c\to 0$, the flow is almost entirely in regions II and IV. Using equations (83) and (88), we obtain

$$\chi^{\mathrm{II,IV}}(v,c) = -I^-(v,c)-I^-(-v,c) = -\left[f(v/2)+\frac{c^2}{4}f''(v/2)\right]\ln\left(\frac{c_0^2}{c^2}\right)+m(v)+O(c^2), \tag{93}$$

where $m(v) = q(v) + q(-v)$ is a function of v alone, and therefore

$$t = \frac{1}{2c}\frac{\partial \chi^{\mathrm{II,IV}}}{\partial c} = \frac{f(v/2)}{c^2} - \frac{f''(v/2)}{4}\ln\left(\frac{c_0^2}{c^2}\right) + O(1),$$
$$x - vt = -\frac{\partial \chi^{\mathrm{II,IV}}}{\partial v} = \frac{f'(v/2)}{2}\ln\left(\frac{c_0^2}{c^2}\right) + O(1). \tag{94}$$

Finally, in the leading approximation, we can rewrite (94) as

$$\frac{\lambda(x,t)}{\lambda_0} = \frac{x_0}{c_0 t} g\left(\frac{x}{2tc_0}\right), \qquad v(x,t) = \frac{x}{t}, \quad \text{for } t \to \infty, \tag{95}$$

where $f(z) = c_0 x_0 g(z/c_0)$ and

$$g(z) = \frac{2}{\pi}\int_0^{\bar{\lambda}_0^{-1}(z^2)} \sqrt{\bar{\lambda}_0(\bar{x}) - z^2}\,\mathrm{d}\bar{x}. \tag{96}$$

Here $\bar{\lambda}_0(\bar{x}) = \lambda_0(x/x_0)/\lambda_0$ is the scaled initial line density profile. One can readily verify that the density profile given by (95) is correctly normalized, and that $g(-z) = g(z)$.

5. Examples with different initial density profiles

In this section, we apply the formalism developed in sections 2–4 to several examples with different initial density profiles.

5.1. Parabolic density profile

As a first example, we consider here the case of an initial parabolic density profile for $\lambda(x, 0) = \lambda_0(x)$ with

$$\frac{\lambda_0(x)}{\lambda_0} = \left[1 - \left(\frac{x}{x_0}\right)^2\right]\Theta(|x| < x_0). \tag{97}$$

5.1.1. Cold beam. For a cold beam, $c^2 = \lambda\,\mathrm{d}w/\mathrm{d}\lambda = c_g^2(\lambda/\lambda_0)$. Substituting (97) into (96) and integrating, we obtain

$$f(z) = \frac{c_0 x_0}{2}\left[1 - \left(\frac{z}{c_0}\right)^2\right]\Theta(z < c_0). \tag{98}$$

Next we substitute (98) into the integral

$$I^-(a,b) = \int_1^\infty \frac{\mathrm{d}t}{\sqrt{t^2-1}} f(tc - v/2) = \frac{c_0 x_0}{(a+b)^2}\int_1^b \frac{\mathrm{d}t}{\sqrt{t^2-1}}(b-t)(a+t)$$
$$= \frac{c_0 x_0}{(a+b)^2}\left[\sqrt{b^2-1}(b-2a) + [(2ab-1)\ln(b+\sqrt{b^2-1})\right], \tag{99}$$

and define

$$I^{+}(a,b)=\int_{1}^{\infty}\frac{\mathrm{d}t}{\sqrt{t^{2}-1}}f(tc+v/2)=I^{-}(b,a), \tag{100}$$

where we have introduced the new variables

$$b=\frac{2c_{0}+v}{2c},\qquad a=\frac{2c_{0}-v}{2c}. \tag{101}$$

In terms of the new variables, it follows that

$$\begin{aligned}\chi^{\mathrm{I,III}}(a,b)&=I^{+}(a,b)-I^{-}(a,b)\\&=\frac{c_{0}x_{0}}{(a+b)^{2}}\left[(a-2b)\sqrt{a^{2}-1}-(b-2a)\sqrt{b^{2}-1}+(2ab-1)\ln\frac{a+\sqrt{a^{2}-1}}{b+\sqrt{b^{2}-1}}\right],\end{aligned} \tag{102}$$

$$\begin{aligned}\chi^{\mathrm{II,IV}}(a,b)&=-I^{+}(a,b)-I^{-}(a,b)\\&=-\frac{c_{0}x_{0}}{(a+b)^{2}}\left[(a-2b)\sqrt{a^{2}-1}+(b-2a)\sqrt{b^{2}-1}+(2ab-1)\ln\frac{a+\sqrt{a^{2}-1}}{b-\sqrt{b^{2}-1}}\right].\end{aligned} \tag{103}$$

By introducing the scaled variables $\bar{x}=x/x_{0}$, $\bar{t}=tc_{0}/x_{0}$ and $\bar{\chi}=\chi/x_{0}c_{0}$, we can rewrite equation (8) as

$$\bar{t}=-\frac{(a+b)^{2}}{8}\left[a\frac{\partial}{\partial a}+b\frac{\partial}{\partial b}\right]\bar{\chi}, \tag{104}$$

$$\bar{x}=-\frac{(a^{2}-b^{2})}{4}\left[a\frac{\partial}{\partial a}+b\frac{\partial}{\partial b}\right]\bar{\chi}-\frac{(a+b)}{4}\left[\frac{\partial}{\partial b}-\frac{\partial}{\partial a}\right]\bar{\chi}. \tag{105}$$

Finally, substituting equations (102) and (103) into (104) and (105), and using equations (101), we obtain after some lengthy algebra the solution in regions I and III,

$$\bar{t}=\frac{(1-\bar{v})}{4\bar{c}^{2}}\sqrt{(1+\bar{v})^{2}-\bar{c}^{2}}-\frac{(1+\bar{v})}{4\bar{c}^{2}}\sqrt{(1-\bar{v})^{2}-\bar{c}^{2}}+\frac{1}{4}\ln\frac{1+\bar{v}+\sqrt{(1+\bar{v})^{2}-\bar{c}^{2}}}{1-\bar{v}+\sqrt{(1-\bar{v})^{2}-\bar{c}^{2}}}, \tag{106}$$

$$\bar{x}=\frac{(\bar{c}^{2}+\bar{v}-\bar{v}^{2})\sqrt{(1+\bar{v})^{2}-\bar{c}^{2}}+(\bar{c}^{2}-\bar{v}-\bar{v}^{2})\sqrt{(1-\bar{v})^{2}-\bar{c}^{2}}}{2\bar{c}^{2}}, \tag{107}$$

and in regions II and IV,

$$\bar{t}=\frac{(1+\bar{v})}{4\bar{c}^{2}}\sqrt{(1-\bar{v})^{2}-\bar{c}^{2}}+\frac{(1-\bar{v})}{4\bar{c}^{2}}\sqrt{(1+\bar{v})^{2}-\bar{c}^{2}}+\frac{1}{4}\ln\frac{1+\bar{v}+\sqrt{(1+\bar{v})^{2}-\bar{c}^{2}}}{1-\bar{v}-\sqrt{(1-\bar{v})^{2}-\bar{c}^{2}}}, \tag{108}$$

$$\bar{x}=\frac{(\bar{c}^{2}+\bar{v}-\bar{v}^{2})\sqrt{(1+\bar{v})^{2}-\bar{c}^{2}}-(\bar{c}^{2}-\bar{v}-\bar{v}^{2})\sqrt{(1-\bar{v})^{2}-\bar{c}^{2}}}{2\bar{c}^{2}}. \tag{109}$$

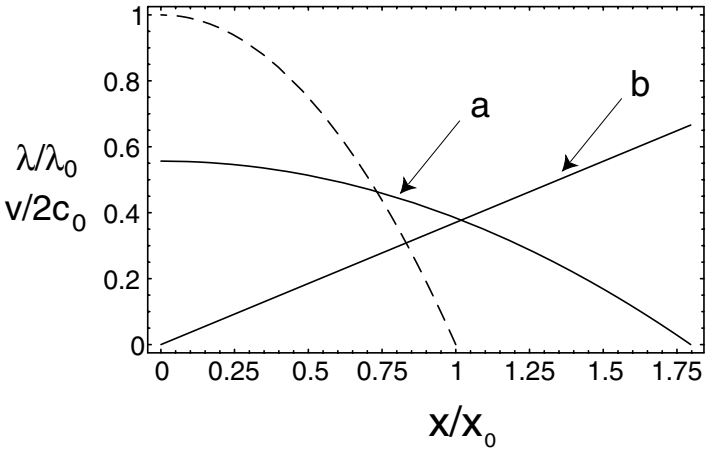

Figure 5. Plots of (a) the normalized density $\lambda(x, t)/\lambda_0$, and (b) the normalized flow velocity $v/2c_0$, at $c_0t/x_0 = 1$ as functions of x for a cold beam. The initial density profile (dotted line) is given by equation (97).

Here we have introduced the definitions $\bar{v} = v/2c_0$ and $\bar{c} = c/c_0$. Equations (106)–(109) can be easily inverted. The result is

$$\frac{v}{c_0} = 2\frac{x}{x_0}\left(\frac{2f}{1+f^2}\right)^2\left(\frac{1-f^2}{1+f^2}\right), \tag{110}$$

$$\frac{c}{c_0} = \frac{2f}{1+f^2}\sqrt{1-\left[\frac{x}{x_0}\right]^2\left(\frac{2f}{1+f^2}\right)^4}, \tag{111}$$

$$\left(\frac{v}{1-f^2}\right)^2 + \left(\frac{c}{f}\right)^2 = \left(\frac{2c_0}{1+f^2}\right)^2, \tag{112}$$

$$\frac{\lambda}{\lambda_0} = \left(\frac{2f}{1+f^2}\right)^2\left[1-\left(\frac{x}{x_0}\right)^2\left(\frac{2f}{1+f^2}\right)^4\right], \tag{113}$$

where $0 < f \leqslant 1$ is the solution of the transcendental equation

$$\bar{t} = \frac{1-f^4}{8f^2} - \frac{1}{2}\ln f. \tag{114}$$

The solutions in (110)–(114) describe the familiar self-similar solution [92]–[94] for a parabolic density profile and is plotted in figure 5. Using (95) and (98), we obtain the asymptotic solution as $t \to \infty$

$$\frac{\lambda(x,t)}{\lambda_0} = \bar{c}^2 = \frac{x_0}{2c_0t}\left[1-\left(\frac{x}{2tc_0}\right)^2\right], \qquad v(x,t) = \frac{x}{t}, \quad \text{for } t \to \infty. \tag{115}$$

The exact solution given by (113) and the asymptotic solution given by (115) are compared in figure 6 (curve b) for $c_0t/x_0 = 50$.

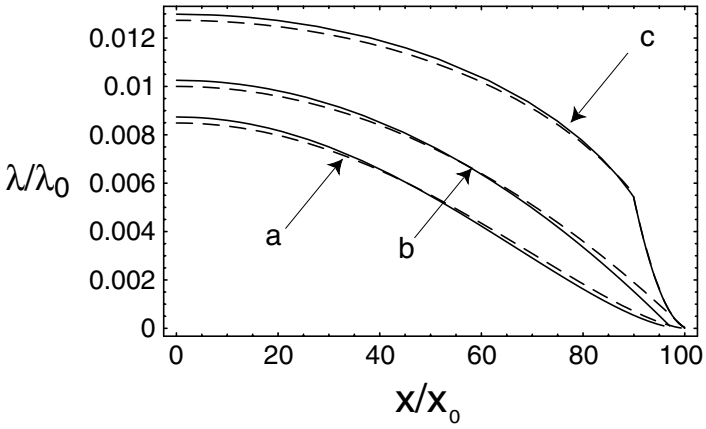

Figure 6. Plots of the normalized density $\lambda(x, t)/\lambda_0$ as a function of x for a cold beam at $c_0 t/x_0 = 50$. The solid lines are the exact solutions. The dotted lines are the approximate solutions given by equation (95). The initial profiles are given by (a) equation (125), (b) equation (97), and (c) equation (143).

5.1.2. Pressure-dominated beam. For a pressure-dominated beam, $c^2 = \lambda\, \mathrm{d}w/\mathrm{d}\lambda = c_p^2(\lambda/\lambda_0)^2$ and therefore the initial profile for $x_0(c)$ is given by $x_0(c)/x_0 = \sqrt{1 - c/c_0}$. Using equation (97) and equations (74) and (75) we obtain the implicit solution in regions I and II,

$$\bar{c} + \bar{v} = 1 - [\bar{x} - (\bar{v} + \bar{c})\bar{t}]^2, \tag{116}$$

$$\bar{c} - \bar{v} = 1 - [\bar{x} - (\bar{v} - \bar{c})\bar{t}]^2, \tag{117}$$

and in regions III and IV,

$$\bar{c} + \bar{v} = 1 - [\bar{x} - (\bar{v} + \bar{c})\bar{t}]^2, \tag{118}$$

$$\bar{v} - \bar{c} = 1 - [\bar{x} - (\bar{v} - \bar{c})\bar{t}]^2. \tag{119}$$

Solving equations (116)–(119) for $\bar{c}(\bar{x}, \bar{t})$ and $\bar{v}(\bar{x}, \bar{t})$, we obtain

$$\bar{c} = \frac{1}{4\bar{t}^2}\left[\sqrt{1 + 4\bar{t}^2 + 4\bar{x}\bar{t}} + \sqrt{1 + 4\bar{t}^2 - 4\bar{x}\bar{t}} - 2\right], \tag{120}$$

$$\bar{v} = \frac{\bar{x}}{\bar{t}} + \frac{1}{4\bar{t}^2}\left[\sqrt{1 + 4\bar{t}^2 - 4\bar{x}\bar{t}} - \sqrt{1 + 4\bar{t}^2 + 4\bar{x}\bar{t}}\right], \tag{121}$$

for regions I and II ($0 < \bar{x} < 1,\ 0 < \bar{t}$), and

$$\bar{c} = \frac{1}{2\bar{t}^2}\sqrt{1 + 4\bar{t}^2 - 4\bar{x}\bar{t}}, \tag{122}$$

$$\bar{v} = \frac{\bar{x}}{\bar{t}} - \frac{1}{2\bar{t}^2}, \tag{123}$$

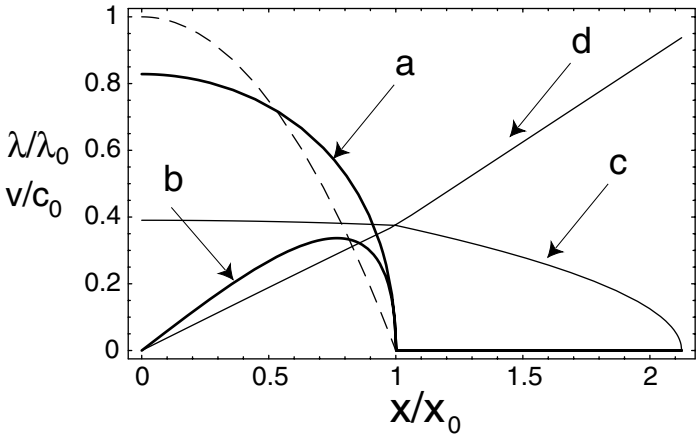

Figure 7. Plots of the normalized density $\lambda(x, t)/\lambda_0$ for $c_0t/x_0 = 0.5$ in (a) and for $c_0t/x_0 = 2$ in (c), and the flow velocity v/c_0 for $c_0t/x_0 = 0.5$ in (b) and for $c_0t/x_0 = 2$ in (d), as functions of x for a pressure-dominated beam. The initial density profile (dotted line) is given by equation (97).

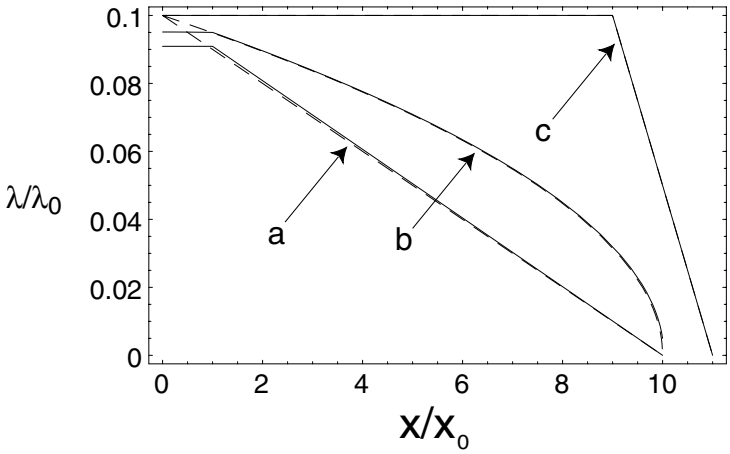

Figure 8. Plots of the normalized density $\lambda(x, t)/\lambda_0$ as a function of x for a pressure-dominated beam at $c_0t/x_0 = 10$. The solid lines are the exact solutions. The dotted lines are the approximate solutions given by equation (64). The initial profiles are given by (a) equation (125), (b) equation (97), and (c) equation (143).

for regions III and IV ($1 < \bar{x},\ 1/2 < \bar{t}$). The solutions (equations (120)–(123)) are illustrated in figure 7. Using (64) we obtain the asymptotic solution as $t \to \infty$

$$\frac{\lambda(x, t)}{\lambda_0} = \bar{c} = \frac{x_0}{c_0 t}\sqrt{1 - \frac{x}{c_0 t}}, \qquad v(x, t) = \frac{x}{t}, \quad \text{for } t \to \infty. \tag{124}$$

The exact solution given by (122) and asymptotic solution given by (124) are compared in figure 8 (curve b) for $c_0t/x_0 = 10$.

5.2. Linear density profile

The next example we consider corresponds to the initial linear density profile

$$\frac{\lambda_0(x)}{\lambda_0} = \left(1 - \left|\frac{x}{x_0}\right|\right)\Theta(|x| < x_0). \tag{125}$$

5.2.1. Cold beam. Here we repeat the intermediate steps of the previous example. For a cold beam, $c^2 = \lambda\, \mathrm{d}w/\mathrm{d}\lambda = c_g^2(\lambda/\lambda_0)$. Substituting (125) into (96) and integrating, we obtain

$$f(z) = \frac{4c_0x_0}{3\pi}\left[1 - \left(\frac{z}{c_0}\right)^2\right]^{3/2}\Theta(z < c_0). \tag{126}$$

Next we substitute (126) into the integral

$$I^-(a,b) = \int_1^\infty \frac{\mathrm{d}t}{\sqrt{t^2-1}} f(tc - v/2) = \frac{32}{3\pi}\frac{c_0x_0}{(a+b)^3}\int_1^b \frac{\mathrm{d}t}{\sqrt{t^2-1}}[(b-t)(a+t)]^{3/2}, \tag{127}$$

and define

$$I^+(a,b) = \int_1^\infty \frac{\mathrm{d}t}{\sqrt{t^2-1}} f(tc + v/2) = I^-(b,a), \tag{128}$$

where a and b are introduced in (101). By introducing the new integration variable α defined by

$$\sin(\alpha) = \sqrt{\frac{(t-1)(b+1)}{(t+1)(b-1)}}, \tag{129}$$

the integral in (127) can be expressed as

$$\frac{I^-(a,b)}{x_0c_0} = \frac{64}{3\pi}\sqrt{\frac{b-1}{b+1}}\frac{[(b-1)(a+1)]^{3/2}}{(a+b)^3}\int_0^{\pi/2}\mathrm{d}\alpha\,\frac{\cos^4(\alpha)[1-k^2p^2\sin^2(\alpha)]^{3/2}}{[1-k^2\sin^2(\alpha)]^4}, \tag{130}$$

where $k^2 = (b-1)/(b+1)$ and $p^2 = (a-1)/(a+1)$. The integral in (130) can be expressed in terms of elliptic integrals. Finally, using the definitions $\chi^{\mathrm{I,III}} = I^-(b,a) - I^-(a,b)$ and $\chi^{\mathrm{II,IV}} = -I^-(a,b) - I^-(b,a)$, and using (101), (104), and (105), we obtain after some lengthy algebra the solution in regions I and III,

$$\bar{t} = \frac{8}{\pi}\frac{\bar{v}\bar{c}}{\sqrt{(1+\bar{c})^2-\bar{v}^2}}\left[\Pi\left(\frac{1+\bar{v}-\bar{c}}{1+\bar{v}+\bar{c}}, \frac{(1-\bar{c})^2-\bar{v}^2}{(1+\bar{c})^2-\bar{v}^2}\right)\right.$$
$$\left. + \Pi\left(\frac{1-\bar{v}-\bar{c}}{1-\bar{v}+\bar{c}}, \frac{(1-\bar{c})^2-\bar{v}^2}{(1+\bar{c})^2-\bar{v}^2}\right) - K\left(\frac{(1-\bar{c})^2-\bar{v}^2}{(1+\bar{c})^2-\bar{v}^2}\right)\right] = 2\bar{v}, \tag{131}$$

$$\bar{x} = \frac{4}{\pi}\frac{(1+2\bar{v}^2-\bar{c}^2)\bar{c}}{\sqrt{(1+\bar{c})^2-\bar{v}^2}}\left[\Pi\left(\frac{1+\bar{v}-\bar{c}}{1+\bar{v}+\bar{c}}, \frac{(1-\bar{c})^2-\bar{v}^2}{(1+\bar{c})^2-\bar{v}^2}\right)\right.$$
$$\left. + \Pi\left(\frac{1-\bar{v}-\bar{c}}{1-\bar{v}+\bar{c}}, \frac{(1-\bar{c})^2-\bar{v}^2}{(1+\bar{c})^2-\bar{v}^2}\right) - K\left(\frac{(1-\bar{c})^2-\bar{v}^2}{(1+\bar{c})^2-\bar{v}^2}\right)\right] = 1 + 2\bar{v}^2 - \bar{c}^2, \tag{132}$$

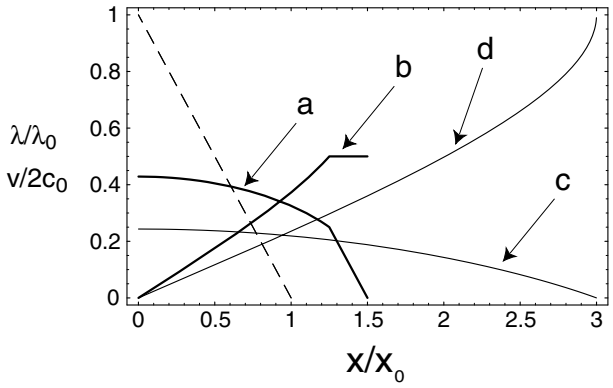

Figure 9. Plots of the normalized density $\lambda(x, t)/\lambda_0$ for $c_0t/x_0 = 0.5$ in (a) and for $c_0t/x_0 = 2$ in (c), and the flow velocity v/c_0 for $c_0t/x_0 = 0.5$ in (b) and for $c_0t/x_0 = 2$ in (d), as functions of x for a pressure-dominated beam. The initial density profile (dotted line) is given by equation (97).

and in regions II and IV,

$$\bar{t} = \frac{4}{3\pi}\frac{1}{\bar{c}^2\sqrt{(1+\bar{c})^2-\bar{v}^2}}\left[6\bar{c}^3\bar{v}\left\{\Pi\left(\frac{1+\bar{v}-\bar{c}}{1+\bar{v}+\bar{c}},\frac{(1-\bar{c})^2-\bar{v}^2}{(1+\bar{c})^2-\bar{v}^2}\right)\right.\right.$$
$$\left.-\Pi\left(\frac{1-\bar{v}-\bar{c}}{1-\bar{v}+\bar{c}},\frac{(1-\bar{c})^2-\bar{v}^2}{(1+\bar{c})^2-\bar{v}^2}\right)\right\}+2\bar{c}(2\bar{c}^2+\bar{v}^2-3\bar{c}\bar{v}^2+\bar{c}-1)K\left(\frac{(1-\bar{c})^2-\bar{v}^2}{(1+\bar{c})^2-\bar{v}^2}\right)$$
$$\left.-((1+\bar{c})^2-\bar{v}^2)(2\bar{c}^2+\bar{v}^2-1)E\left(\frac{(1-\bar{c})^2-\bar{v}^2}{(1+\bar{c})^2-\bar{v}^2}\right)\right], \tag{133}$$

$$\bar{x} = \frac{2}{3\pi}\frac{1}{\bar{c}^2\sqrt{(1+\bar{c})^2-\bar{v}^2}}\left[6\bar{c}^3(1-\bar{c}^2+2\bar{v}^2)\left\{\Pi\left(\frac{1+\bar{v}-\bar{c}}{1+\bar{v}+\bar{c}},\frac{(1-\bar{c})^2-\bar{v}^2}{(1+\bar{c})^2-\bar{v}^2}\right)\right.\right.$$
$$\left.-\Pi\left(\frac{1-\bar{v}-\bar{c}}{1-\bar{v}+\bar{c}},\frac{(1-\bar{c})^2-\bar{v}^2}{(1+\bar{c})^2-\bar{v}^2}\right)\right\}$$
$$-2\bar{c}\bar{v}(4-4\bar{v}^2+\bar{c}(2+\bar{c}-3\bar{c}^2+6\bar{v}^2))K\left(\frac{(1-\bar{c})^2-\bar{v}^2}{(1+\bar{c})^2-\bar{v}^2}\right)$$
$$\left.+\bar{v}((1+\bar{c})^2-\bar{v}^2)(4+\bar{c}^2-4\bar{v}^2)E\left(\frac{(1-\bar{c})^2-\bar{v}^2}{(1+\bar{c})^2-\bar{v}^2}\right)\right], \tag{134}$$

where $\bar{v} = v/2c_0$, $\bar{c} = c/c_0$, $\bar{x} = x/x_0$ and $\bar{t} = tc_0/x_0$. Here, K, E and Π are the complete elliptic integrals of the first, second, and third kind, respectively [102]. The solution to the expansion problem for the linear density profile (125) is given by (131)–(134) and is illustrated in figure 9. Using equations (131) and (132), we can rewrite the solution in regions I and III as

$$v = \frac{c_0^2}{x_0}t, \tag{135}$$

$$\frac{\lambda}{\lambda_0} = 1 + \frac{c_0^2}{2x_0^2}t^2 - \left|\frac{x}{x_0}\right|. \tag{136}$$

This simple flow with uniform acceleration in regions I and III exists only until $t = t_{cr} = 2x_0/c_0$. At this time the characteristic Q overtakes the edge of the beam, and the flow for $t > t_{cr}$ is entirely in regions II and IV and is given by (133) and (134). Using (95) and (126) we obtain the asymptotic solution as $t \to \infty$

$$\frac{\lambda(x,t)}{\lambda_0} = \bar{c}^2 = \frac{4x_0}{3\pi c_0 t}\left[1 - \left(\frac{x}{2tc_0}\right)^2\right]^{3/2}, \qquad v(x,t) = \frac{x}{t}, \quad \text{for } t \to \infty. \tag{137}$$

The exact solution given by (133) and (134) and the asymptotic solution given by (137) are compared in figure 6 (curve a) for $c_0 t/x_0 = 50$.

5.2.2. Pressure-dominated beam. For a pressure-dominated beam, $c^2 = \lambda\, \mathrm{d}w/\mathrm{d}\lambda = c_p^2(\lambda/\lambda_0)^2$. Hence, for the linear density profile in (125), the initial profile for $x_0(c)$ is

$$\frac{x_0(c)}{x_0} = \left[1 - \left(\frac{c}{c_0}\right)\right]\Theta(c < c_0), \tag{138}$$

where x_0 is the initial beam half-length, and c_0 is the speed of sound at $x = 0$. Substituting (138) into (59)–(62), we obtain the solution in region I,

$$\bar{c} = \frac{1-\bar{x}}{1-\bar{t}^2}, \qquad \bar{v} = \bar{t}\frac{1-\bar{x}}{1-\bar{t}^2}, \quad \text{for } 0 < \bar{t} < 1, \quad \bar{t} < \bar{x} < 1, \tag{139}$$

in region II,

$$\bar{c} = \frac{1}{1+\bar{t}}, \qquad \bar{v} = \frac{\bar{x}}{1+\bar{t}}, \quad \text{for } 0 < \bar{t}, \quad 0 < x < \min(\bar{t}, 1), \tag{140}$$

and in region IV,

$$\bar{c} = \frac{\bar{t}-\bar{x}}{\bar{t}^2-1}, \qquad \bar{v} = \frac{\bar{x}\bar{t}-1}{\bar{t}^2-1}, \quad \text{for } 1 < \bar{t}, \quad 1 < x < \bar{t}. \tag{141}$$

Region III has disappeared. Indeed, using (61) we obtain $\bar{x} = 1$ and $\bar{t} = 1$, so that the entire region consists of just one point. The corresponding solutions (equations (139)–(141)) are illustrated in figure 10. Using equations (64) and (138) we obtain the asymptotic solution as $t \to \infty$

$$\frac{\lambda(x,t)}{\lambda_0} = \bar{c} = \frac{x_0}{c_0 t}\left(1 - \frac{x}{c_0 t}\right), \qquad v(x,t) = \frac{x}{t}, \quad \text{for } t \to \infty. \tag{142}$$

The exact solution given by (141) and the asymptotic solution given by (142) are compared in figure 8 (line a) for $c_0 t/x_0 = 10$.

5.3. Flat-top density profile

As discussed in section 2, the general flow consists of regions where either a simple wave solution (equation (20)) or a general solution (solution of (14) together with (8)) is applicable.

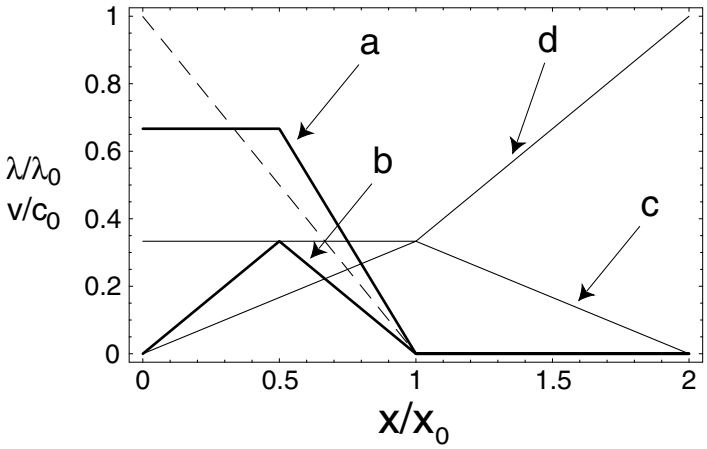

Figure 10. Plots of the normalized density $\lambda(x, t)/\lambda_0$ for $c_0t/x_0 = 0.5$ in (a) and for $c_0t/x_0 = 2$ in (c), and the flow velocity v/c_0 for $c_0t/x_0 = 0.5$ in (b) and for $c_0t/x_0 = 2$ in (d), as functions of x for a pressure-dominated beam. The initial density profile (dotted line) is given by equation (125).

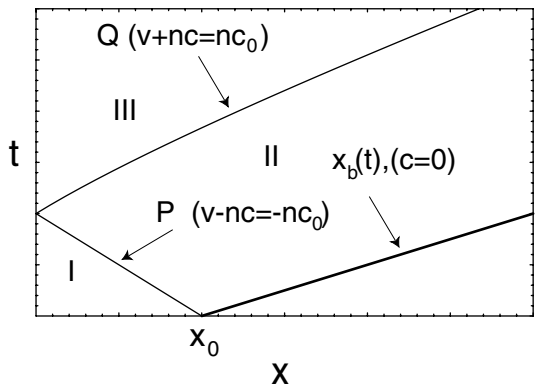

Figure 11. The area in the (x, t) plane occupied by the three regions of flow.

Up to now we have considered flows with no simple wave regions. This is guaranteed provided the initial density profile is smooth everywhere except at the beam edge where the sound speed is zero, $c_0(x_0) = 0$. Here, we consider an example with an initial flat-top density profile, and a corresponding discontinuity in density at the beam edge, i.e.,

$$\frac{\lambda_0(x)}{\lambda_0} = \Theta(|x| < x_0). \tag{143}$$

This problem is equivalent to the one-dimensional expansion of a uniform-density gas into vacuum in a vessel in which the end walls are instantly removed. The (x, t) plane is shown in figure 11. The flow consists of three regions. In region I the gas is at rest, and the information that the walls have been removed, which is carried by the C_- characteristic P into the gas, does not reach this region. Region II is the region occupied by a simple rarefaction wave which is centred at $t = 0$ and $x = x_0$ in the (x, t) plane, and is described by the simple wave solution in (20). Region

III is the region of interference of this wave and and its reflection from the origin (or another rarefaction wave coming from the other end of the gas region). This region is described by the general solution in (14) together with (8). Regions II and III are separated by the C_+ characteristic Q. On this characteristic the boundary condition in (27) holds. To determine the function $f(v)$ in (20) and (27), we note that for $t = 0$, $x = x_0$ and therefore $f(v) = x_0 = \text{const}$. Also note that the characteristics C_+ bring the value of the Riemann invariant $J_+ = v + nc = nc_0 = \text{const}$ to all points of region II. Therefore, the solution in region II is given by

$$c = \frac{n}{n+1}c_0 - \frac{1}{n+1}\frac{x - x_0}{t}, \tag{144}$$

$$v = \frac{n}{n+1}c_0 + \frac{n}{n+1}\frac{x - x_0}{t}, \tag{145}$$

where $n = 1, 2$, and the boundary condition for χ on the separating characteristic Q where $v + nc = nc_0$ is given by

$$\chi|_{v+nc=nc_0} = -x_0 v. \tag{146}$$

The second boundary condition (equation (42)) is given by

$$\left(\frac{\partial \chi}{\partial v}\right)_{v=0} = 0. \tag{147}$$

5.3.1. Cold beam. The function χ satisfying the boundary condition in (147) is given by

$$\chi(v, c) = -\int_1^\infty \frac{\mathrm{d}t}{\sqrt{t^2 - 1}}[f(tc + v/2) + f(tc - v/2)]. \tag{148}$$

Using (146) and (148), we obtain the integral equation for the function f,

$$x_0 v = \int_1^\infty \frac{\mathrm{d}t}{\sqrt{t^2 - 1}}\{f[(c_0 - v/2)t - v/2] + f[(c_0 - v/2)t + v/2]\}. \tag{149}$$

By setting $v = 0$ in (149) we note that the function f has the form $f(t) = g(t)\Theta(t < c_0)$. Substituting this expression for $f(t)$ into (149), and changing the integration variable to $x = t(1 - v/2c_0) - v/2c_0$, we obtain the integral equation for the function g,

$$\int_{1-v/c_0}^1 \frac{\mathrm{d}x\, g(c_0 x)}{\sqrt{(x+1)(x - [1 - v/c_0])}} = v x_0. \tag{150}$$

Changing the integration variables in (150) according to $y = \sqrt{x+1}$, and introducing the new function $p(y) \equiv g[c_0(2y^2 - 1)]$, we obtain an integral equation of the Abel type,

$$\int_a^1 \frac{\mathrm{d}y\, p(y)}{\sqrt{y^2 - a^2}} = c_0 x_0 \left(1 - a^2\right)\Theta(a < 1), \tag{151}$$

where $a = \sqrt{1 - v/2c_0}$. Equation (151) is easily solved using the Abel transform described in appendix A. We obtain

$$p(y) = c_0 x_0 \frac{4}{\pi} y\sqrt{1 - y^2}. \tag{152}$$

Finally, since $g(x) = p(\sqrt{1/2 + x/2c_0})$, we obtain

$$f(x) = c_0 x_0 \frac{2}{\pi}\sqrt{1 - \left(\frac{x}{c_0}\right)^2}\,\Theta(x < c_0). \tag{153}$$

Next we substitute (153) into the integral

$$I^-(a, b) = \int_1^\infty \frac{\mathrm{d}t}{\sqrt{t^2 - 1}} f(tc - v/2) = \frac{4}{\pi}\frac{c_0 x_0}{(a + b)}\int_1^b \frac{\mathrm{d}t}{\sqrt{t^2 - 1}}[(b - t)(a + t)]^{1/2}, \tag{154}$$

and define

$$I^+(a, b) = \int_1^\infty \frac{\mathrm{d}t}{\sqrt{t^2 - 1}} f(tc + v/2) = I^-(b, a), \tag{155}$$

where a and b are introduced in (101). By introducing the new integration variable α defined by

$$\sin(\alpha) = \sqrt{\frac{(t - 1)(b + 1)}{(t + 1)(b - 1)}}, \tag{156}$$

the integral in (154) can be rewritten as

$$\frac{I^-(a, b)}{x_0 c_0} = \frac{8}{\pi}\sqrt{\frac{b - 1}{b + 1}}\frac{[(b - 1)(a + 1)]^{1/2}}{(a + b)}\int_0^{\pi/2} \mathrm{d}\alpha \frac{\cos^2(\alpha)[1 - k^2 p^2 \sin^2(\alpha)]^{1/2}}{[1 - k^2 \sin^2(\alpha)]^2}, \tag{157}$$

where $k^2 = (b - 1)/(b + 1)$ and $p^2 = (a - 1)/(a + 1)$. The integral in (157) can be expressed in terms of elliptic integrals. Finally, using the definition $\chi = -I^-(b, a) - I^-(a, b)$, and making use of (101), (104) and (105), we obtain after some lengthy algebra the solution in region III,

$$\bar{t} = \frac{2}{\pi\bar{c}^2\sqrt{(1 + \bar{c})^2 - \bar{v}^2}}\left\{[(1 + \bar{c})^2) - \bar{v}^2]E\left[\frac{(1 - \bar{c})^2 - \bar{v}^2}{(1 + \bar{c})^2 - \bar{v}^2}\right] - 2\bar{c}K\left[\frac{(1 - \bar{c})^2 - \bar{v}^2}{(1 + \bar{c})^2 - \bar{v}^2}\right]\right\}, \tag{158}$$

$$\bar{x} = \frac{4}{\pi\bar{c}^2\sqrt{(1 + \bar{c})^2 - \bar{v}^2}}\left\{\bar{v}[(1 + \bar{c})^2) - \bar{v}^2]E\left[\frac{(1 - \bar{c})^2 - \bar{v}^2}{(1 + \bar{c})^2 - \bar{v}^2}\right] - \bar{v}\bar{c}(2 + \bar{c})K\left[\frac{(1 - \bar{c})^2 - \bar{v}^2}{(1 + \bar{c})^2 - \bar{v}^2}\right]\right.$$
$$\left. + \Pi\left[\frac{1 - \bar{c} - \bar{v}}{1 + \bar{c} - \bar{v}}, \frac{(1 - \bar{c})^2 - \bar{v}^2}{(1 + \bar{c})^2 - \bar{v}^2}\right] - \Pi\left[\frac{1 - \bar{c} + \bar{v}}{1 + \bar{c} + \bar{v}}, \frac{(1 - \bar{c})^2 - \bar{v}^2}{(1 + \bar{c})^2 - \bar{v}^2}\right]\right\}, \tag{159}$$

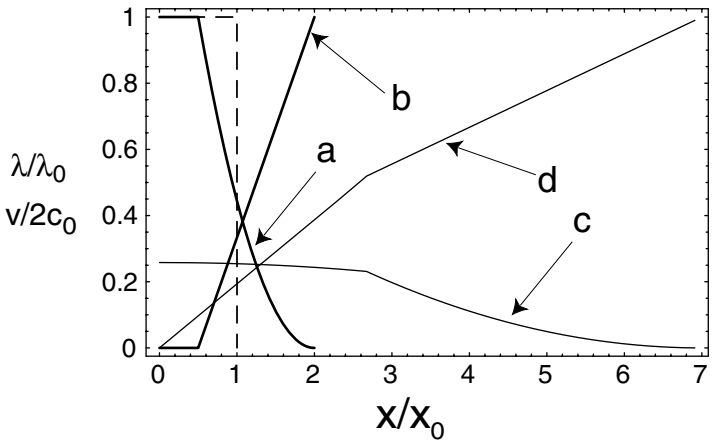

Figure 12. Plots of the normalized density $\lambda(x, t)/\lambda_0$ for $c_0t/x_0 = 0.5$ in (a) and for $c_0t/x_0 = 3$ in (c), and the flow velocity $v/2c_0$ for $c_0t/x_0 = 0.5$ in (b) and for $c_0t/x_0 = 3$ in (d), as functions of x for a cold beam. The initial density profile (dotted line) is given by equation (143).

where $\bar{v} = v/2c_0$, $\bar{c} = c/c_0$, $\bar{x} = x/x_0$ and $\bar{t} = tc_0/x_0$. Here, K, E and Π are the complete elliptic integrals of the first, second, and third kinds, respectively [102]. The solution in region II is given by equations (144) and (145) with $n = 2$, i.e.,

$$\bar{c} = \frac{1}{3}\left(2 - \frac{\bar{x} - 1}{\bar{t}}\right), \tag{160}$$

$$\bar{v} = \frac{1}{3}\left(1 + \frac{\bar{x} - 1}{\bar{t}}\right). \tag{161}$$

Using equations (160) and (161) we can determine the trajectory of the beam edge and the characteristics Q and P. At the beam edge, $c = 0$, and therefore from (160) we obtain $x_b(t) = x_0 + 2c_0t$. On the characteristic P, $v = 0$, and from (161) we obtain $x_P(t) = x_0 - c_0t$. On the characteristic Q, $\mathrm{d}x/\mathrm{d}t = v + c = 4c_0/3 + (x - x_0)/3t$. Integrating this equation, we obtain

$$x_Q(t) = x_0 + c_0t\left(2 - \frac{3}{(c_0t/x_0)^{2/3}}\right). \tag{162}$$

The solutions given by (158)–(161) are illustrated in figure 12. Using equations (95) and (153) we obtain the asymptotic solution in region III $[0 < x < x_Q(t)]$ as $t \to \infty$

$$\frac{\lambda(x, t)}{\lambda_0} = \bar{c}^2 = \frac{2x_0}{\pi c_0 t}\sqrt{1 - \left(\frac{x}{2tc_0}\right)^2}, \qquad v(x, t) = \frac{x}{t}, \quad \text{for } t \to \infty. \tag{163}$$

The asymptotic solution in region II $[x_Q(t) < x < x_b(t)]$ is still given by (160) and (161). The exact solution given by (158)–(161) and the asymptotic solution given by (163) and (160) are compared in figure 6 (curve c) for $c_0t/x_0 = 50$.

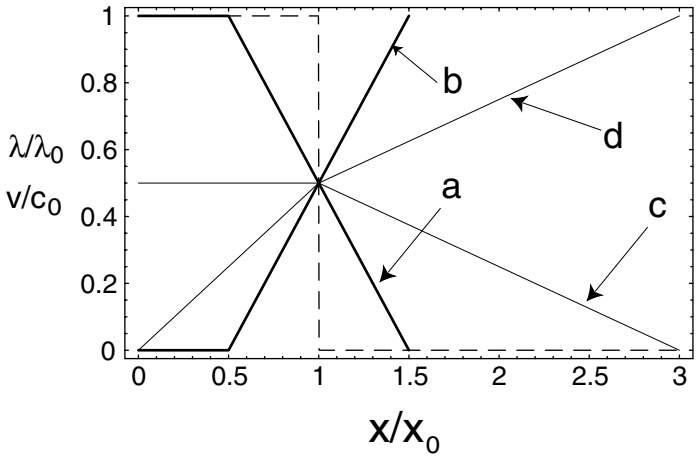

Figure 13. Plots of the normalized density $\lambda(x, t)/\lambda_0$ for $c_0t/x_0 = 0.5$ in (a) and for $c_0t/x_0 = 2$ in (c), and the flow velocity v/c_0 for $c_0t/x_0 = 0.5$ in (b) and for $c_0t/x_0 = 2$ in (d), as functions of x for a pressure-dominated beam. The initial density profile (dotted line) is given by equation (143).

5.3.2. Pressure-dominated beam. The function χ satisfying the boundary condition in (147) is given by

$$\chi(v, c) = f(c - v) + f(c + v). \tag{164}$$

Using the boundary condition on the characteristic Q, it follows that $\chi = -x_0v$ for $v + c = c_0$, and we obtain

$$-vx_0 = f(c_0 - 2v) + f(c_0). \tag{165}$$

Substituting $v = 0$ into (165), we find that $f(c_0) = 0$ and therefore $f(c_0 - 2v) = -vx_0$, or $f(x) = (x_0/2)(x - c_0)$. Using (164), we obtain

$$\chi(v, c) = x_0(c - c_0), \tag{166}$$

and using (8), we obtain $t = x_0/c$ and $x - vt = 0$. Therefore, the solution in region III is given by

$$\bar{c} = \frac{1}{\bar{t}}, \qquad \bar{v} = \frac{\bar{x}}{\bar{t}}, \quad \text{for } 1 < \bar{t}, \quad 0 < \bar{x} < \bar{t} - 1. \tag{167}$$

The solution in region II is given by equations (144) and (145) with $n = 1$, i.e.,

$$\bar{c} = \frac{1}{2}\left(1 - \frac{\bar{x} - 1}{\bar{t}}\right), \qquad \bar{v} = \frac{1}{2}\left(1 + \frac{\bar{x} - 1}{\bar{t}}\right), \quad |\bar{t} - 1| < \bar{x} < 1 + \bar{t}. \tag{168}$$

In region I, the gas is undisturbed: $\bar{c} = 1$ and $\bar{v} = 0$, for $0 < \bar{x} < 1 - \bar{t}$ and $\bar{t} < 1$. The characteristic Q is given by the equation $\bar{x}_Q(t) = \bar{t} - 1$, and the beam edge is given by $\bar{x}_b(t) = 1 + \bar{t}$. The solutions given by (167) and (168) are illustrated in figure 13. Since χ in (166) is a linear function of c and is independent of v, the asymptotic ($t \to \infty$) solution coincides with the exact solution in (167).

5.4. Continuous density profile (no sharp edge boundary)

Up to this point we have considered flows which do not become multi-valued (in the absence of dissipation) and therefore are time-reversible [89, 90]. For such flows, the compression problem is equivalent to the time-reversed expansion problem. In this section, we consider an example of fluid flow which becomes multi-valued. For simplicity, we consider here a beam without sharp edges in which $\lambda_0(x)$ decreases to zero monotonically as $x \to \pm\infty$. In particular, we consider the initial density profile given by

$$\frac{\lambda_0(x)}{\lambda_0} = \frac{1}{\cosh^2(x/x_0)}. \tag{169}$$

Expanding flows with initially smooth profiles extending to $x \to \pm\infty$ such as in (169) are entirely in regions I and II. Indeed regions I and II are separated from regions III and IV by the C_- characteristic P with $v - nc = -nc_0 = 0$ $(n = 1, 2)$. However, for profiles such as (169), $c_0(x) > 0$ for all $|x| < \infty$, and therefore the entire region $|x| < \infty$ maps into regions I and II in the (v, c) plane (see figure 3). As a result, the solution for the flow is given by equations (59) and (60) for pressure-dominated beams, and by (86) and (88), with $f(z)$ defined in (82) for cold beams.

5.4.1. Cold beam. For a cold beam, $c^2 = \lambda\,\mathrm{d}w/\mathrm{d}\lambda = c_g^2(\lambda/\lambda_0)$, and therefore $c/c_0 = 1/\cosh(x/x_0)$. Substituting (169) into (96) and integrating, we obtain

$$f(z) = x_0 c_0 \left(1 - \frac{|z|}{c_0}\right) \Theta(z < c_0). \tag{170}$$

Substituting (170) into the integral for $I^-(a, b)$ and integrating, we obtain

$$I^-(a, b) = \int_1^\infty \frac{\mathrm{d}t}{\sqrt{t^2 - 1}} f(tc - v/2) = -\frac{2x_0 c_0}{a + b}[\sqrt{b^2 - 1} - b \ln(b + \sqrt{b^2 - 1})], \tag{171}$$

and

$$I^+(a, b) = \int_1^\infty \frac{\mathrm{d}t}{\sqrt{t^2 - 1}} f(tc + v/2) = I^-(b, a), \tag{172}$$

where a and b are introduced in (101). Using the definitions $\chi^{\mathrm{I}} = I^-(b, a) - I^-(a, b)$ and $\chi^{\mathrm{II}} = -I^-(b, a) - I^-(a, b)$, and making use of (101), (104) and (105), we obtain the solution in region I,

$$\bar{t} = \frac{\sqrt{(1 + \bar{v})^2 - \bar{c}^2} - \sqrt{(1 - \bar{v})^2 - \bar{c}^2}}{2\bar{c}^2}, \tag{173}$$

$$\bar{x} = \bar{v}\frac{\sqrt{(1 + \bar{v})^2 - \bar{c}^2} - \sqrt{(1 - \bar{v})^2 - \bar{c}^2}}{\bar{c}^2} + \frac{1}{2} \ln \left[\frac{1 + \bar{v} + \sqrt{(1 + \bar{v})^2 - \bar{c}^2}}{1 - \bar{v} - \sqrt{(1 - \bar{v})^2 - \bar{c}^2}}\right], \tag{174}$$

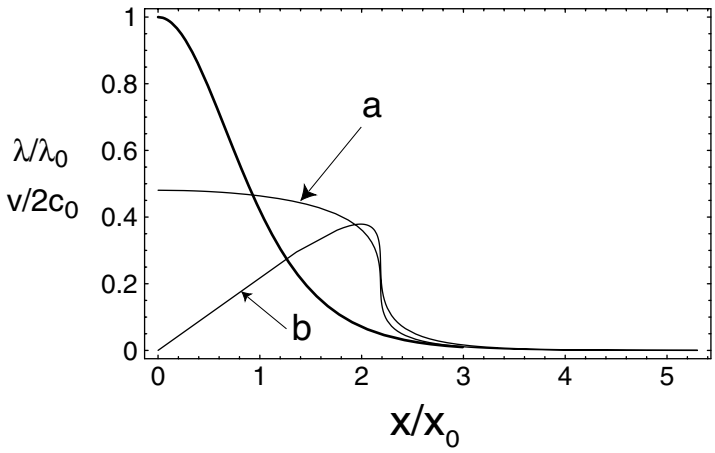

Figure 14. Plots of the normalized density $\lambda(x, t)/\lambda_0$ in (a) and flow velocity $v/2c_0$ in (b) at $c_0t/x_0 = 1.5$ as functions of x for a cold beam. The initial density profile (thick solid line) is given by equation (169).

and in region II,

$$\bar{t} = \frac{\sqrt{(1+\bar{v})^2 - \bar{c}^2} + \sqrt{(1-\bar{v})^2 - \bar{c}^2}}{2\bar{c}^2}, \tag{175}$$

$$\bar{x} = \bar{v}\frac{\sqrt{(1+\bar{v})^2 - \bar{c}^2} + \sqrt{(1-\bar{v})^2 - \bar{c}^2}}{\bar{c}^2} + \frac{1}{2}\ln\left[\frac{1+\bar{v}+\sqrt{(1+\bar{v})^2 - \bar{c}^2}}{1-\bar{v}+\sqrt{(1-\bar{v})^2 - \bar{c}^2}}\right]. \tag{176}$$

Equations (173)–(176) can be partially inverted to give

$$\bar{v}^2 = \frac{\bar{t}^2\bar{\lambda}^2(\bar{t}^2\bar{\lambda}^2 + \bar{\lambda} - 1)}{(\bar{t}^2\bar{\lambda}^2 - 1)}, \tag{177}$$

where

$$\bar{\lambda} = \frac{1}{\cosh^2(\bar{x} - 2\bar{v}\bar{t})} - \frac{\bar{v}^2}{\sinh^2(\bar{x} - 2\bar{v}\bar{t})}, \tag{178}$$

and $\bar{\lambda} = \lambda/\lambda_0 = \bar{c}^2$. The solutions given by (177) and (178) are illustrated in figure 14. As evident from (177), $(\partial\bar{v}/\partial\bar{\lambda})_t > 0$ in some regions, which means that the regions with higher density accelerated faster than the regions with lower density, and eventually multi-valued flow is formed (see figure 14). This is unlike the previous examples where $(\partial\bar{v}/\partial\bar{\lambda})_t < 0$ for all t, and there was no multi-valued flow.

5.4.2. Pressure-dominated beam. For a pressure-dominated beam, $c^2 = \lambda\, \mathrm{d}w/\mathrm{d}\lambda = c_p^2(\lambda/\lambda_0)^2$. Using (169) and (74) and (75), we obtain the implicit solution in regions I and II,

$$\bar{c}(x, t) = \frac{1}{2}\left\{\frac{1}{\cosh^2[\bar{x} - (\bar{v} + \bar{c})\bar{t}]} + \frac{1}{\cosh^2[\bar{x} - (\bar{v} - \bar{c})\bar{t}]}\right\}, \tag{179}$$

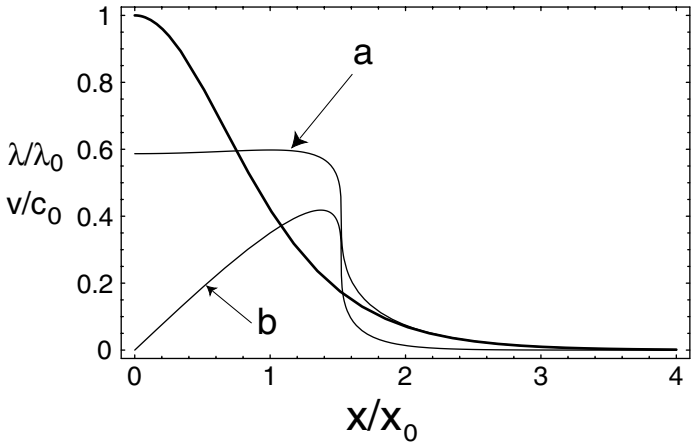

Figure 15. Plots of the normalized density $\lambda(x, t)/\lambda_0$ in (a) and flow velocity v/c_0 in (b) at $c_0 t/x_0 = 1.3$ as functions of x for a pressure-dominated beam. The initial density profile (thick solid line) is given by equation (169).

$$\bar{v}(x, t) = \frac{1}{2}\left\{\frac{1}{\cosh^2[\bar{x} - (\bar{v} + \bar{c})\bar{t}]} - \frac{1}{\cosh^2[\bar{x} - (\bar{v} - \bar{c})\bar{t}]}\right\}. \tag{180}$$

The solutions given by (179) and (180) are illustrated in figure 15.

6. Beam shaping

In this section we consider the beam-shaping problem referred to in section 1. That is, given an initial line density profile $\Lambda_{in}(x)$ at time $t = 0$ and final line density profile $\Lambda_f(x)$ at time $t = T_{shape}$, what are the initial and finial velocity profiles, $V_{in}(x)$ and $V_f(x)$ respectively. The beam-shaping stage is necessary to prepare the beam density profile for the final drift compression discussed in previous sections. Here, as in previous sections, we analyse the time-reversed problem. Therefore, the initial density profile $\Lambda_{in}(x)$ for the time-reversed problem is given by (95) and (96) for a cold beam, or by (64) for a pressure-dominated beam, and the final density profile $\Lambda_f(x)$ illustrated schematically in figure 1. During the beam shaping stage, the longitudinal pressure and electric field are negligible and the beam dynamics is governed by free convection described by

$$\left(\frac{\partial}{\partial t} + v\frac{\partial}{\partial x}\right) v = 0, \tag{181}$$

$$\frac{\partial x}{\partial v} - v\frac{\partial t}{\partial v} + \lambda\frac{\partial t}{\partial \lambda} = 0. \tag{182}$$

Here, (182) follows from multiplying (12) by $\mathrm{d}w/\mathrm{d}\lambda$, and is equivalent to (1). Equation (181) implies that the function v is constant along the characteristic given by $\mathrm{d}x/\mathrm{d}t = v$, which therefore corresponds to straight lines given by

$$x = vt + f(v) \quad \text{or} \quad v(x, t) = V[x - v(x, t)t], \tag{183}$$

where $v(x, 0) = V(x)$ and $V[f(v)] = v$. Equation (183) gives a general solution to (181) for the velocity profile $v(x, t)$. Substituting (183) into (182), we obtain $t = -f'(v) + q(v)/\lambda$, where $q(v)$ is an arbitrary function of v. Using the initial condition that at $t = 0$, $\lambda = \lambda_0(v)$, we obtain the solution to (182), $\lambda = \lambda_0(v)/[1 + t/f'(v)]$. Note that $1/f'(v) \equiv V'[f(v)] = V'(x - vt)$, and $\lambda_0(v) = \lambda_0[V(x - vt)] \equiv \Lambda(x - vt)$, where $\Lambda(x)$ is the initial density profile as a function of x. Therefore, the solution to (181) and (182) is given by [93]

$$v(x, t) = V[x - v(x, t)t], \tag{184}$$

$$\lambda(x, t) = \frac{\Lambda[x - v(x, t)t]}{1 + tV'[x - v(x, t)t]}. \tag{185}$$

Setting $t = T_{shape}$ and introducing now the function $U_{in}(x) = x + T_{shape}V_{in}(x)$, we can rewrite (184) as $V_f(x) = v(x, T_{shape}) = V_{in}[x - V_f(x)T_{shape}] = \{U_{in}[x - V_f(x)T_{shape}] - [x - V_f(x)T_{shape}]\}/T_{shape}$, or equivalently, $x = U_{in}[x - V_f(x)T_{shape}]$. Finally, using the definition of the function $U_{in}(x)$, we can rewrite (184) and (185) in a compact and manifestly time-reversible form giving the final formal solution to the beam shaping problem, i.e.,

$$V_f(x) = \frac{x - U_f(x)}{T_{shape}}, \qquad V_{in}(x) = \frac{U_{in}(x) - x}{T_{shape}}, \tag{186}$$

$$\int_0^{U_{in}(x)} \Lambda_f(\bar{u})\,\mathrm{d}\bar{u} = \int_0^x \Lambda_{in}(\bar{x})\,\mathrm{d}\bar{x} \quad \text{or} \quad \int_0^x \Lambda_f(\bar{x})\,\mathrm{d}\bar{x} = \int_0^{U_f(x)} \Lambda_{in}(\bar{u})\,\mathrm{d}\bar{u}. \tag{187}$$

Here, $U_f(x) = U_{in}^{-1}(x)$ is the inverse of the function $U_{in}(x)$ such that $U_f[U_{in}(x)] \equiv x$, and we have assumed that $\Lambda_f(-x) = \Lambda_f(x)$ and $\Lambda_{in}(-x) = \Lambda_{in}(x)$. Examples applying results in (186) and (187) can be found in [93].

7. Conclusions

To summarize, we have studied the longitudinal drift compression of an intense charged-particle beam using a one-dimensional warm-fluid model. We have reformulated the drift-compression problem as the time-reversed expansion problem of the beam with arbitrary line density profile and zero velocity profile. We have obtained exact analytical solutions to the expansion problem for the two important cases corresponding to a cold beam, and a pressure-dominated beam, using a general formalism which reduces the system of warm-fluid equations to a linear second-order partial differential equation. We obtained simple approximate analytical formulas connecting the initial and final line density profile and flow velocity profile for these two cases. The asymptotic velocity profiles are linear in both cases, and correspond to free expansion as $t \to \infty$. The scaled density profile for a pressure-dominated beam far from the compression point was shown to be the functional inverse of the compressed density profile in (64). For a cold beam, the profiles are connected by the Abel transform (equations (95) and (96)). The general solution has been illustrated for parabolic, linear, and flat-top initial (compressed) line density profiles. For the case of a parabolic density profile, we have recovered the familiar self-similar solution [92]–[94]. We have also illustrated the formation of multi-valued flow with the exactly solvable example in (169), and identified the conditions for smooth, single-valued compression.

Acknowledgments

This research was supported by the US Department of Energy. It is a pleasure to acknowledge the benefit of useful discussions with Igor Kaganovich and Hong Qin.

Appendix A. Abel transform

Here we use the following definition of the Abel transform

$$f(z) = A[g(z)] = 2\int_z^\infty \frac{g(x)x\,\mathrm{d}x}{\sqrt{x^2 - z^2}}. \tag{A.1}$$

The inverse Abel transform is given by

$$g(x) = A^{-1}[f(x)] = -\frac{1}{\pi}\int_x^\infty \frac{\mathrm{d}f(z)}{\mathrm{d}z}\frac{\mathrm{d}z}{\sqrt{z^2 - x^2}}. \tag{A.2}$$

The fact that (A.2) is indeed the inverse of the Abel transform in (A.1) can be checked by direct substitution of (A.2) into (A.1). Changing the order of integration leads to

$$f(z) = -\frac{1}{\pi}\int_z^\infty \frac{2x\,\mathrm{d}x}{\sqrt{x^2 - z^2}}\int_x^\infty \frac{\mathrm{d}f(t)}{\mathrm{d}t}\frac{\mathrm{d}t}{\sqrt{t^2 - x^2}} = -\frac{1}{\pi}\int_z^\infty \mathrm{d}t\frac{\mathrm{d}f(t)}{\mathrm{d}t}\int_z^t \frac{2x\,\mathrm{d}x}{\sqrt{t^2 - x^2}\sqrt{x^2 - z^2}}. \tag{A.3}$$

Making the change of variables, $\sin(q) = \sqrt{x^2 - z^2}/\sqrt{t^2 - z^2}$, the final integral in (A.3) is evaluated to be

$$\int_z^t \frac{2x\,\mathrm{d}x}{\sqrt{t^2 - x^2}\sqrt{x^2 - z^2}} = \pi, \tag{A.4}$$

and (A.3) becomes

$$f(z) = -\int_z^\infty \mathrm{d}t\frac{\mathrm{d}f(t)}{\mathrm{d}t} = f(z) - f(\infty). \tag{A.5}$$

Therefore, for functions $f(z)$ such that $f(\infty) = 0$, (A.5) is an identity.

References

[1] Davidson R C and Qin H 2001 *Physics of Intense Charged Particle Beams in High Energy Accelerators* (Singapore: World Scientific) and references therein
[2] Reiser M 1994 *Theory and Design of Charged Particle Beams* (New York: Wiley)
[3] Lawson J D 1988 *The Physics of Charged-Particle Beams* (New York: Oxford Science Publications)
[4] Chao A W 1993 *Physics of Collective Beam Instabilities in High Energy Accelerators* (New York: Wiley)
[5] Edwards D A and Syphers M J 1993 *An Introduction to the Physics of High-Energy Accelerators* (New York: Wiley)
[6] Kapchinskij I M and Vladimirskij V V 1959 *Proc. Int. Conf. on High Enegy Accelerators and Instrumentation* (Geneva: CERN Scientific Information Service) p 274

[7] Gluckstern R L 1971 *Proc. Proton Linear Accelerator Conf.* (*Batavia, IL*) ed M R Tracy (Batavia, IL: National Accelerator Laboratory) p 811
[8] Wang T-S and Smith I 1982 *Part. Accel.* **12** 247
[9] Hofmann J, Laslett L J, Smith L and Haber I 1983 *Part. Accel.* **13** 145
[10] Struckmeier J, Klabunde J and Reiser M 1984 *Part. Accel.* **15** 47
[11] Hofmann I and Struckmeier J 1987 *Part. Accel.* **21** 69
[12] Struckmeier J and Hofmann I 1992 *Part. Accel.* **39** 219
[13] Brown N and Reiser M 1995 *Phys. Plasmas* **2** 965
[14] Davidson R C and Qin H 1999 *Phys. Rev. ST Accel. Beams* **2** 114401
[15] Gluckstern R L, Cheng W-H and Ye H 1995 *Phys. Rev. Lett.* **75** 2835
[16] Davidson R C and Chen C 1998 *Part. Accel.* **59** 175
[17] Chen C, Pakter R and Davidson R C 1997 *Phys. Rev. Lett.* **79** 225
[18] Chen C and Davidson R C 1994 *Phys. Rev.* E **49** 5679
[19] Davidson R C, Lee W W and Stoltz P 1998 *Phys. Plasmas* **5** 279
[20] Davidson R C 1998 *Phys. Rev. Lett.* **81** 991
[21] Davidson R C 1998 *Phys. Plasmas* **5** 3459
[22] Stoltz P, Davidson R C and Lee W W 1999 *Phys. Plasmas* **6** 298
[23] Lee W W, Qian Q and Davidson R C 1997 *Phys. Lett.* A **230** 347
[24] Qian Q, Lee W W and Davidson R C 1997 *Phys. Plasmas* **4** 1915
[25] Tzenov S I and Davidson R C 2002 *Phys. Rev. ST Accel. Beams* **5** 021001
[26] Davidson R C and Qin H 2001 *Phys. Rev. ST Accel. Beams* **4** 104401
[27] Davidson R C, Qin H and Channell P J 1999 *Phys. Rev. ST Accel. Beams* **2** 074401
Davidson R C, Qin H and Channell P J 2000 *Phys. Rev. ST Accel. Beams* **3** 029901
[28] Davidson R C, Friedman A, Celata C M, Welch D R *et al* 2002 *Laser Part. Beams* **20** 377
[29] Harris E G 1959 *Phys. Rev. Lett.* **2** 34
[30] Startsev E A, Davidson R C and Qin H 2002 *Phys. Plasmas* **9** 3138
[31] Startsev E A, Davidson R C and Qin H 2002 *Laser Part. Beams* **20** 585
[32] Startsev E A, Davidson R C and Qin H 2003 *Phys. Rev. ST Accel. Beams* **6** 084401
[33] Startsev E A and Davidson R C 2003 *Phys. Rev. ST Accel. Beams* **6** 044401
[34] Kishek R A, O'Shea P G and Reiser M 2000 *Phys. Rev. Lett.* **85** 4514
[35] Haber J, Friedman A, Grote D P, Lund S M and Kishek R A 1999 *Phys. Plasmas* **6** 2254
[36] Friedman A, Grote D P and Haber I 1992 *Phys. Fluids* B **4** 2203
[37] Weibel E S 1959 *Phys. Rev. Lett.* **2** 83
[38] Startsev E A and Davidson R C 2003 *Phys. Plasmas* **10** 4829
[39] Davidson R C, Hammer D A, Haber I and Wagner C E 1972 *Phys. Fluids* **15** 317
[40] Lee R and Lampe M 1973 *Phys. Rev. Lett.* **31** 1390
[41] Kapetanakos C A 1974 *Appl. Phys. Lett.* **25** 484
[42] Honda M, Meyer-ter-Vehn J and Pukhov A 2000 *Phys. Rev. Lett.* **85** 2128
[43] Neil V K and Sessler A M 1965 *Rev. Sci. Instrum.* **36** 429
[44] Lee E P 1981 *Proc. Linear Accelerator Conf., Los Alamos National Laboratory Report* LA-9234-C, pp 263–5
[45] Lee E P 1992 *Part. Accel.* **37** 307
[46] Davidson R C, Qin H and Shvets G 2003 *Phys. Rev. ST Accel. Beams* **6** 104402
[47] Neuffer D, Colton B, Fitzgerald D, Hardek T, Hutson R, Macek R, Plum M, Thiessen H and Wang T S 1992 *Nucl. Instrum. Methods Phys. Res.* A **321** 1
[48] Macek R J *et al* 2001 *Proc. Particle Accelerator Conf.* vol 1, p 688
[49] Davidson R C, Qin H and Wang T-S 1999 *Phys. Lett.* A **252** 213
[50] Davidson R C, Qin H, Stoltz P H and Wang T-S 1999 *Phys. Rev. ST Accel. Beams* **2** 054401
[51] Davidson R C and Qin H 2000 *Phys. Lett.* A **270** 177
[52] Qin H, Davidson R C and Lee W W 2000 *Phys. Rev. ST Accel. Beams* **3** 084401 and 109901
[53] Davidson R C and Uhm H S 2001 *Phys. Lett.* A **285** 88

[54] Qin H, Davidson R C, Startsev E A and Lee W W 2003 *Laser Part. Beams* **21** 21
[55] Wang T-S, Channell P J, Macek R J and Davidson R C 2003 *Phys. Rev. ST Accel. Beams* **6** 014204
[56] Qin H, Startsev E A and Davidson R C 2003 *Phys. Rev. ST Accel. Beams* **6** 014401
[57] Qin H 2003 *Phys. Plasmas* **10** 2708
[58] Lee E P 1978 *Phys. Fluids* **21** 1327
[59] Lauer E J, Briggs R J, Fesendon T J, Hester R E and Lee E P 1978 *Phys. Fluids* **21** 1344
[60] Rosenbluth M N 1960 *Phys. Fluids* **3** 932
[61] Uhm H S and Lampe M 1980 *Phys. Fluids* **23** 1574
[62] Uhm H S and Lampe M 1981 *Phys. Fluids* **24** 1553
[63] Fernsler R F, Slinker S P, Lampe M and Hubbard R F 1995 *Phys. Plasmas* **2** 4338 and references therein
[64] Uhm H S and Davidson R C 2003 *Phys. Rev. ST Accel. Beams* **6** 034204
[65] Uhm H S, Davidson R C and Kaganovich I D 2001 *Phys. Plasmas* **8** 4637
[66] Joyce G and Lampe M 1983 *Phys. Fluids* **26** 3377
[67] Uhm H S and Davidson R C 1980 *Phys. Fluids* **23** 1586
[68] Kaganovich I D, Shvets G, Startsev E and Davidson R C 2001 *Phys. Plasmas* **8** 4180
[69] Kaganovich I, Startsev E A and Davidson R C 2002 *Laser Part. Beams* **20** 497
[70] Rose D V, Ottinger P F, Welch D R, Oliver B V and Olson C L 1999 *Phys. Plasmas* **6** 4094
[71] Welch D R, Rose D V, Oliver B V, Genoni T C, Olson C L and Yu S S 2002 *Phys. Plasmas* **9** 2344
[72] Hofmann I 1982 *Z. Naturforsch.* A **37** 939
[73] Hofmann I 1985 *Laser Part. Beams* **3** 1
[74] Boine-Frankenheim O, Hofmann I and Rumolo G 1999 *Phys. Rev. Lett.* **82** 3256
[75] Spentzouris L K, Ostiguy J-F and Colestock P L 1996 *Phys. Rev. Lett.* **76** 620
[76] Spentzouris L K, Colestock P L and Bhat C 1999 *Proc. Particle Accelerator Conf.* vol 1, p 114
[77] Fedele R, Miele G, Palumbo L and Vaccaro V G 1993 *Phys. Lett.* A **179** 407
[78] Schamel H 1997 *Phys. Rev. Lett.* **79** 2811
[79] Schamel H and Fedele R 2000 *Phys. Plasmas* **7** 3421
[80] Hofmann A 1977 *CERN Report* No. 77-13
[81] Neuffer D 1980 *Part. Accel.* **11** 23
[82] Allen C K, Brown N and Reiser M 1994 *Part. Accel.* **45** 149
[83] Sharp W M, Friedman A and Grote D P 1996 *Fusion Eng. Des.* **32** 201
[84] Wang J G, Suk H, Wang D X and Reiser M 1994 *Phys. Rev. Lett.* **72** 2029
[85] Davidson R C and Startsev E A 2004 *Phys. Rev. ST Accel. Beams* **7** 024401
[86] Davidson R C and Strasburg S 2000 *Phys. Plasmas* **7** 2657
[87] Lund S M and Davidson R C 1998 *Phys. Plasmas* **5** 3028
[88] Davidson R C, Qin H, Tzenov S I and Startsev E A 2002 *Phys. Rev. ST Accel. Beams* **5** 084402
[89] Sack Ch and Schamel H 1987 *Phys. Rep.* **156** 311
[90] Schamel H 2004 *Phys. Rep.* **392** 279
[91] Landau L D and Lifshitz E M 1987 *Fluid Mechanics* (Oxford: Pergamon)
[92] Qin H, Davidson R C, Barnard J J and Lee E P 2003 *Proc. Particle Accelerator Conf.* p 2658
[93] Qin H and Davidson R C 2002 *Phys. Rev. ST Accel. Beams* **5** 03441
[94] Qin H and Davidson R C 2002 *Laser Part. Beams* **20** 565
[95] Haber I 1982 *Proc. Symp. on Accelerator Aspects of Heavy Ion Fusion (Darmstadt)* (Darmstadt: GSI) p 372
[96] Hofmann I and Bozsik I 1982 *Proc. Symp. on Accelerator Aspects of Heavy Ion Fusion (Darmstadt)* (Darmstadt: GSI) p 362
[97] Bisognano J, Lee E P and Mark J W-K 1985 *LLNL Report* No. 3-28
[98] Ho D D-M, Brandon S T and Lee E P 1991 *Part. Accel.* **35** 15
[99] de Hoon M J L 2001 *PhD Thesis* University of California, Berkeley
[100] Lee E P and Barnard J J 2001 *Proc. Particle Accelerator Conf. (Chicago)* p 2928
[101] Qin H, Jun C, Davidson R C and Heitzenroeder P 2001 *Proc. Particle Accelerator Conf. (Chicago)* p 1761
[102] Abromowitz M and Stegun I 1972 *Handbook of Mathematical Functions* (New York: Dover)